

ACCEPTED MANUSCRIPT • OPEN ACCESS

## A review of chemical looping reforming technologies for hydrogen production: recent advances and future challenges

To cite this article before publication: Rouzbeh Ramezani *et al* 2023 *J. Phys. Energy* in press <https://doi.org/10.1088/2515-7655/acc4e8>

### Manuscript version: Accepted Manuscript

Accepted Manuscript is “the version of the article accepted for publication including all changes made as a result of the peer review process, and which may also include the addition to the article by IOP Publishing of a header, an article ID, a cover sheet and/or an ‘Accepted Manuscript’ watermark, but excluding any other editing, typesetting or other changes made by IOP Publishing and/or its licensors”

This Accepted Manuscript is © 2023 The Author(s). Published by IOP Publishing Ltd.

As the Version of Record of this article is going to be / has been published on a gold open access basis under a CC BY 4.0 licence, this Accepted Manuscript is available for reuse under a CC BY 4.0 licence immediately.

Everyone is permitted to use all or part of the original content in this article, provided that they adhere to all the terms of the licence <https://creativecommons.org/licenses/by/4.0>

Although reasonable endeavours have been taken to obtain all necessary permissions from third parties to include their copyrighted content within this article, their full citation and copyright line may not be present in this Accepted Manuscript version. Before using any content from this article, please refer to the Version of Record on IOPscience once published for full citation and copyright details, as permissions may be required. All third party content is fully copyright protected and is not published on a gold open access basis under a CC BY licence, unless that is specifically stated in the figure caption in the Version of Record.

View the [article online](#) for updates and enhancements.

# **A Review of Chemical Looping Reforming Technologies for Hydrogen Production: recent advances and future challenges**

Rouzbeh Ramezani\*, Luca Di Felice, Fausto Gallucci\*

Sustainable Process Engineering, Department of Chemical Engineering and Chemistry, Eindhoven University of Technology, De Rondom 70, 5612 AP Eindhoven, the Netherlands

## **Abstract**

Faced with increasingly serious energy and global warming, it is critical to put forward an alternative non-carbonaceous fuel. In this regard, hydrogen appears as the ultimate clean fuel for power and heat generation, and as an important feedstock for various chemical and petrochemical industries. The chemical looping reforming (CLR) concept, is an emerging technique for the conversion of hydrocarbon fuels into high-quality hydrogen via the circulation of oxygen carriers which allows a decrease in CO<sub>2</sub> emissions. In this review, a comprehensive evaluation and recent progress in glycerol, ethanol and methane reforming for hydrogen production are presented. The key elements for a successful CLR process are studied and the technical challenges to achieve high-purity hydrogen along with the possible solutions are also assessed. As product quality, cost and the overall efficiency of the process can be influenced by the oxygen carrier materials used, noteworthy attention is given to the most recent development in this field. The use of Ni, Fe, Cu, Ce, Mn and Co-based material as potential oxygen carriers under different experimental conditions for hydrogen generation from different feedstock by CLR is discussed. Furthermore, the recent research conducted on the sorption-enhanced reforming process is reviewed and the performance of the various type of CO<sub>2</sub> sorbents such as CaO, Li<sub>2</sub>ZrO<sub>3</sub> and MgO is highlighted.

---

\*Corresponding author: Prof. Fausto Gallucci, E-mail: [f.gallucci@tue.nl](mailto:f.gallucci@tue.nl)

## 1. Introduction

Nowadays, the production of clean energy and the reduction of greenhouse gas emissions have drawn much attention all over the world (Teh et al., 2021)(Teh et al., 2021). In the past few decades, fossil fuels such as petroleum and coal have become the main energy sources that lead to the exponential growth of the CO<sub>2</sub> concentration in the atmosphere from 310 ppm in 1960 to 419 ppm in 2021, resulting in significant environmental concerns (Alam et al., 2020)(Alam et al., 2020). The rise of global temperature, species extinction, sea-level rise, and ocean acidification are some examples of the consequences of anthropogenic greenhouse gases emission into the atmosphere (G. Hu et al., 2016)(G. Hu et al., 2016). Therefore, it is both imperative and critical to develop efficient strategies along with greater reliance on renewable energy to reduce global CO<sub>2</sub> emissions.

The utilization of hydrogen as an alternative to carbon-containing fossil fuels indicates an additional approach to mitigate global warming risks (Wassie et al., 2017)(Wassie et al., 2017). Thanks to its pollution-free characteristics as well as its high heating value and rich resources, hydrogen has great potential to become a promising substitute as a clean energy carrier (van Renssen, 2020)(van Renssen, 2020). On the other hand, hydrogen demand is expected to continually increase with increasing industrialization over time and the world population (Chaubey et al., 2013)(Chaubey et al., 2013).

Although carbon-based fuels supply 85% of the world's energy claim, it is predicted that hydrogen would be responsible for 90% of the world's energy in 2080 which shows its significant role in future energy (Roslan et al., 2020)(Roslan et al., 2020). The food industry, treating metals, chemical manufacturing industry, petroleum refining, glass purification, hydrocracking and fuel cells are the main sectors for hydrogen application (Barreto et al., 2003)(Barreto et al., 2003) (Delparish & Avci, 2016)(Delparish & Avci, 2016). In order to accept hydrogen as a major energy source, it should be produced sustainably and

1  
2  
3  
4  
5  
6  
7  
8  
9  
10  
11  
12  
13  
14  
15  
16  
17  
18  
19  
20  
21  
22  
23  
24  
25  
26  
27  
28  
29  
30  
31  
32  
33  
34  
35  
36  
37  
38  
39  
40  
41  
42  
43  
44  
45  
46  
47  
48  
49  
50  
51  
52  
53  
54  
55  
56  
57  
58  
59  
60

efficiently. Hydrogen is classified into three main classes including blue hydrogen, grey hydrogen and green hydrogen depending on their production approach and raw materials (Atilhan et al., 2021)(Atilhan et al., 2021).

Green hydrogen has a much lower environmental cost compared to grey and blue-based technologies (Baykara, 2018)(Baykara, 2018). In recent years, great effort has been put into advancement in materials, cost and technical issues during producing green hydrogen from renewables that will reduce the cost of production of green hydrogen by up to 70% during the next decade (Atilhan et al., 2021)(Atilhan et al., 2021).

The production of hydrogen can be done using various technologies such as biological processes, photoelectrolysis, water splitting by high-temperature heat, water electrolysis, gasification of coal and biomass, natural gas, or biogas reforming (Iriondo et al., 2008)(Iriondo et al., 2008). Several factors such as system integration options, technological availability, resources and their use, costs, efficiency and environmental impacts should take into account in order to select a hydrogen production method (Ji & Wang, 2021)(Ji & Wang, 2021). Among them, chemical looping techniques are the most promising and innovative platform for hydrogen production and CO<sub>2</sub> capture (P. Wang et al., 2015). Chemical-looping refers to a cycling process that utilizes a solid metal oxide to transfer oxygen from the air to the fuel via redox reactions (Lee et al., 2021). From an energy point of view, chemical looping is a unique approach that can not only convert different feedstocks to various value-added chemicals such as alkene, ammonia, synthesis gas and H<sub>2</sub>/CO with low production cost but also tackle the issue of CO<sub>2</sub> capture (Fan et al., 2015a).

Depending on gas product components and the differences in oxygen originations, this technology can be employed in a wide range of applications such as chemical looping hydrogen generation, chemical looping reforming, chemical looping gasification and chemical looping combustion (Osman et al., 2021).

The keys to a successful implementation of a chemical looping technique are an appropriate selection of oxygen carriers and an effective reactor design which directed the attempts toward the development of oxygen carriers (Fan et al., 2012). Throughout the years, a range of chemical looping technology in different applications have been reviewed by researchers in the literature which mainly focused on the advances of oxygen carriers in an application or chemical looping reforming (CLR) based on a specific feedstock. CLR concept involves oxidation of a fuel via cyclic reduction and oxidation of a solid oxygen carrier. The main advantage of this process is that the heat needed for converting fuel to hydrogen is supplied without costly oxygen production, without mixing of air with carbon containing fuel gases or without using part of the hydrogen generated in the system (de Diego et al., 2009). The heat for the endothermic reduction reactions in fuel reactor is provided by the circulating solids coming from the air reactor at higher temperature meaning no external heat is required.

Another specific advantage of the a-CLR process is the possibility of obtaining pure  $N_2$  at the outlet stream of the air reactor by controlling the amount of air fed into the air reactor (García-Díez et al., 2017). There is less concern with respect to coke formation in CLR because cycles are self-regenerative. However, deactivation can still pose limitations in many oxide systems because of incomplete coke removal (Sastre et al., 2019). Circulating fluidized beds in CLR provides good contact between gas and solids and allows a smooth flow of oxygen-carrier particles between the reactors. One of the key issues regarding system performance in CLR technology development is the selection of oxygen carrier. The carbon deposition of oxygen carriers can cause poor stability which is still a serious challenge in industrial application. Moreover, material deactivation caused by carbon deposition is also one of the main issues. Toxicity and the cost of oxygen carriers may also limit their application (Meshksar et al., 2017).

1  
2  
3  
4  
5  
6  
7  
8  
9  
10  
11  
12  
13  
14  
15  
16  
17  
18  
19  
20  
21  
22  
23  
24  
25  
26  
27  
28  
29  
30  
31  
32  
33  
34  
35  
36  
37  
38  
39  
40  
41  
42  
43  
44  
45  
46  
47  
48  
49  
50  
51  
52  
53  
54  
55  
56  
57  
58  
59  
60

**Table 1** summarizes an overview of studies that have recently been published in the literature in the field of chemical looping. (Masoudi Soltani et al., 2021) reviewed the recent developments in hydrogen production by sorption-enhanced steam methane reforming. The authors presented a discussion on the advancements in catalysts/adsorbents preparation and process optimization. (Roslan et al., 2020) highlighted the recent advances in Ni-based glycerol reforming processes. They discussed the role of nickel as a catalyst in the reforming reactions and the challenges faced by this technology. A brief review of recent findings in the development of oxygen carrier materials for chemical looping was carried out by (Cheng et al., 2018). (Tang et al., 2015) provided a review of the recent advances in oxygen carriers utilized in the chemical-looping reforming of methane. According to reported studies in the literature, it seems that a review paper that comprehensively focuses on the chemical looping reforming system from different feedstocks with an extensive review of oxygen carrier materials and CO<sub>2</sub> sorbents is still missing.

Therefore, in this work, the authors reviewed key technological breakthroughs in the field of chemical looping reforming from a different point of view to provide a comprehensive assessment. The review starts with recent findings on chemical looping reforming based on methane, ethanol and glycerol, followed by their performance and advantages. Major efforts have been made toward main achievements in the characterization and preparation of the most used oxygen carrier materials. Next, the importance of the selection of different CO<sub>2</sub> sorbents was assessed and their results and progress were presented. Finally, the important challenges related to chemical looping reforming systems for high-purity hydrogen production were highlighted.

**Table 1:** List of published review works done on chemical looping technologies.

Ref.	Review description
(Masoudi Soltani et al., 2021)	Recent development in hydrogen production via steam methane reforming
(Roslan et al., 2020)	Recent findings on Ni-based glycerol reforming processes

(Cheng et al., 2018)	A brief overview of development of oxygen carriers for chemical looping systems
(Tang et al., 2015)	A review of oxygen carriers for methane-based chemical looping reforming

---

## 2. Chemical looping reforming

In recent years, various sources such as coal, natural gas and biomass have been considered for CLR technologies. While many feedstocks can be utilized for reforming, methane is preferred for hydrogen production as it has low cost, high availability, high hydrogen-to-carbon ratio and lower byproduct formation in comparison to other starting materials (Alirezaei et al., 2018a). Steam methane reforming is currently the most common and developed technology used for hydrogen production at large scales (García-Labiano et al., 2015a). Although the main experience of obtaining hydrogen by the CLR process is with gaseous fuels, liquid fuels from renewable sources (biomass or biofuels) are becoming more relevant in the last years for reasons of sustainability. Among them, ethanol offers high possibilities due to the large amount available. High hydrogen content, less hazard, safe transport and high heating value are advantages that make ethanol an important candidate for hydrogen production (Vizcaino et al., 2008). Besides ethanol, other bio-source has been proved to be a good feedstock for steam reforming such as glycerol. The selection of glycerol feedstock is based in part on its ready and cheap availability as a by-product of bio-diesel production (Ni et al., 2017).

All hydrocarbon fuels can be used as raw material in the production of hydrogen. Chemical looping reforming can be operated with both liquid and gaseous fuels. The design of fuel-reactor and the type of oxygen carrier strongly depend on fuel type and feed phase. The fluidized bed, moving bed and packed bed reactors were studied in the literature for CLR for liquid, and gaseous fuels (Vos et al., 2020a). The production cost and the purity of produced hydrogen, heat transfer and process control are also important factors in selection of fuel. Reactions and the operating conditions in fuel reactors such as fuel-to-water

ratio, pressure, temperature and contact time vary with feed composition. For example, steam reforming of glycerol involves complex reactions that result in several intermediates affecting the selectivity of the hydrogen. The heats of the reaction depend on the fuel type and the metal oxide used as an oxygen carrier. Both gaseous and liquid fuels in CLR may contain impurities that limit the oxygen transfer capacity, reactivity, and selectivity. To achieve a full conversion of fuel and a long lifetime of the oxygen carrier, it is crucial to select the oxygen carrier depending on the fuel used in the fuel reactor (Porrazzo et al., 2014). A summary of studies performed on chemical looping reforming using different fuels was listed in **Table 2**.

**Table 2:** Summary of chemical looping reforming of various feedstocks studied in the literature

Oxygen carrier	Reactant	Temperature (°C)	H <sub>2</sub> Purity	Reactant conversion	Ref.
CuO-Ni/Al <sub>2</sub> O <sub>3</sub>	Ethanol	500-650	83 %	98-100 %	(Nimmas et al., 2020)
NiO/Al <sub>2</sub> O <sub>3</sub>	Ethanol	600	97 %	82-93 %	(Dou et al., 2018)
NiFe/MgAl	Ethanol	400-700	78 %	100 %	(Saupsor et al., 2021)
Ni/Al <sub>2</sub> O <sub>4</sub>	Ethanol	900	82 %	91 %	(Q. Zhang et al., 2021)
Ni/Al <sub>2</sub> O <sub>3</sub>	Ethanol	600-900	61 %	72 %	(K. Wang, Dou, Jiang, Zhang, et al., 2016)
NiO-CuO/Al <sub>2</sub> O <sub>3</sub>	Ethanol	100-900	N.A.	N.A.	(López Ortiz et al., 2015)
LaSrNiO	Ethanol	650	75-83 %	80-85 %	(Q. Zhang et al., 2017)
CeNi/SBA	Ethanol	200-900	90-95 %	100 %	(K. Wang, Dou, Jiang, Song, et al., 2016)
NiFe <sub>2</sub> O <sub>4</sub>	Ethanol	450	70-80 %	100 %	(Trevisanut et al., 2015)
Ni/CeO <sub>2</sub>	Ethanol	200-800	N.A.	88 %	(Isarapakdeetham et al., 2020)
NiMn <sub>2</sub> O <sub>4</sub>	Ethanol	500-800	N.A.	N.A.	(W. Wang et al., 2017)
LaNiO <sub>3</sub> /MMT	Ethanol	650	70-80 %	87 %	(L. Li et al., 2017)
Ni/CeO <sub>2</sub>	Ethanol	100-600	88 %	80 %	(L. Li et al., 2018)
NiO/Al <sub>2</sub> O <sub>3</sub>	Ethanol	850-950	62 %	100 %	(García-Labiano et al., 2015b)
NiO/MMT	Ethanol	550	60-70 %	70-80 %	(Jiang et al., 2016)
Ir/La <sub>2</sub> O <sub>3</sub>	Ethanol	400-850	90-100 %	N.A.	(Yang et al., 2011)
Ni-Ca/Al <sub>2</sub> O <sub>3</sub>	Ethanol	550-650	N.A.	99 %	(Elias et al., 2013)
Ce-Ni/Fe	Glycerol	200-800	80-90 %	60-80 %	(Luo et al., 2022)
CeNiO	Glycerol	500-650	85 %	60 %	(K. Wang, Dou, Jiang, Song, et al., 2016)
Rh/Al <sub>2</sub> O <sub>3</sub>	Glycerol	550-700	N.A.	93-100 %	(Delparish et al., 2019)



NiO	Glycerol	750-850	60 %	100 %	(Adánez-Rubio et al., 2021)
Fe-Ce-Ni	Glycerol	600-800	80.6 %	70-100 %	(Lu et al., 2021)
Rh/UGSO	Glycerol	650	N.A.	94-100 %	(Alizadeh Sahraei et al., 2021)
Ni-Mg/ATP	Glycerol	400-800	94.7 %	87.9 %	(Qingli et al., 2021)
Ni/Al <sub>2</sub> O <sub>3</sub>	Glycerol	600-750	N.A.	65-95 %	(Tavanarad et al., 2021)
Ni/ZrO <sub>2</sub>	Glycerol	650	94 %	99 %	(Jiang, Li, Bian, Li, Sun, et al., 2018)
Rh-Mg/Al <sub>2</sub> O <sub>4</sub>	Glycerol	300-600	76 %	99.6 %	(Zarei Senseni et al., 2017)
Ni-Co-Cu/Al <sub>2</sub> O <sub>3</sub>	Glycerol	400-750	65 %	80-95 %	(Papageridis et al., 2016)
Ce-Ni/PSNT	Glycerol	650	70-90 %	88 %	(Jiang, Li, Bian, Li, Othman, et al., 2018)
Ni/Al <sub>2</sub> O <sub>3</sub>	Glycerol	500-600	80-95 %	N.A.	(Dou et al., 2014)
Ni/Al <sub>2</sub> O <sub>3</sub>	Glycerol	550	87.9 %	85-98 %	(Ni et al., 2017)
Ni/Al <sub>2</sub> O <sub>3</sub>	Glycerol	450-600	93 %	99 %	(Jiang et al., 2015)
N.A.	Glycerol	350-700	45-55 %	90-96 %	(H. Chen et al., 2011)
Rh-CeO <sub>2</sub> /Al <sub>2</sub> O <sub>3</sub>	Glycerol	400-750	78 %	90 %	(Charisiou et al., 2020)
Ni/Al <sub>2</sub> O <sub>3</sub>	Glycerol	450-650	N.A.	100 %	(Wu et al., 2013)
Ni-Cu-Al	Glycerol	450-650	92.9 %	90.9 %	(C. Wang et al., 2013)
Ni/Al <sub>2</sub> O <sub>3</sub>	Glycerol	400-700	97 %	100 %	(Dou et al., 2009)
Ni/Al <sub>2</sub> O <sub>3</sub>	Glycerol	600-700	65 %	50 %	(Jiang et al., 2020)
LaSrFeO <sub>3</sub>	Methane	850	N.A.	85-88 %	(Sastre et al., 2022)
LaSrMnCoO	Methane	850	65 %	40-78 %	(Yin et al., 2022)
CeFeO <sub>3</sub>	Methane	650-850	80-85 %	70-80 %	(X. Zhang et al., 2020)
Fe <sub>2</sub> O <sub>3</sub> /MgAl <sub>2</sub> O <sub>4</sub>	Methane	900	91-100 %	83-92 %	(J. Hu, Chen, et al., 2021)
NiO/CeZrO <sub>4</sub>	Methane	700	N.A.	52.8 %	(Y. ke Zhang et al., 2021)
Ni/Fe	Methane	800	93%	96 %	(Z. Hu et al., 2021)
Ni-CeO <sub>2</sub> /MgO	Methane	550-700	N.A.	45%	(Khajenoori et al., 2015)
Ni-Cu	Methane	800	70-80%	30%	(J. Huang et al., 2019)
NiO	Methane	650	75-80%	80-87%	(Antzara et al., 2016)
Ni-CeO <sub>2</sub> /Al <sub>2</sub> O <sub>3</sub>	Methane	700	N.A.	95%	(Rahbar Shamskar et al., 2017)
Ni/CeO <sub>2</sub> -IMP	Methane	800	N.A.	90%	(Guerrero-Caballero et al., 2019)
Cu-Ni-Mn	Methane	650	N.A.	99.4%	(Nazari et al., 2021)
LaFe <sub>2</sub> O <sub>3</sub> /Al <sub>2</sub> O <sub>3</sub>	Methane	800-900	N.A.	55%	(Dai et al., 2012)
Fe <sub>2</sub> O <sub>3</sub> /Al <sub>2</sub> O <sub>3</sub>	Methane	700-900	96%	98%	(M. Zhu et al., 2019)
LaSrFeO <sub>6</sub>	Methane	500-900	50-60%	70-85%	(K. Zhao et al., 2019)
Ce <sub>0.5</sub> Fe <sub>0.5</sub> O <sub>2</sub>	Methane	800-900	92%	90-98%	(X. Zhu et al., 2013)
LaFe <sub>0.7</sub> Co <sub>0.3</sub> O <sub>3</sub>	Methane	500-700	50%	85%	(K. Zhao et al., 2016)
Fe/Al <sub>2</sub> O <sub>3</sub>	Methane	600-800	55%	99%	(Spallina, Gallucci, et al., 2016)
NiO	Methane	600-900	>50%	92%	(Spallina et al., 2017)

NiO/CaAl <sub>2</sub> O <sub>3</sub>	Methane	400-900	N.A.	99%	(Alexandros Argyris et al., 2022)
17%Ni/Al <sub>2</sub> O <sub>3</sub>	Methane	600-750	60%	40%	(Martini, Druiff, et al., 2021)
NiO	Methane	450-650	N.A.	90%	(Medrano et al., 2018)
Ni-Ce	Methane	600-800	N.A.	50-61%	(Iglesias et al., 2017)

2.1. Chemical looping reforming of methane

Methane is the main component of natural gas and unconventional gas, and methane reforming is a high-efficiency and low-energy approach to methane utilization to satisfy the global demand for energy (Yin et al., 2022). The chemical looping reforming is similar to chemical looping combustion, but instead of full combustion of methane to generate water, CO<sub>2</sub> and heat, the methane is partially oxidized by an oxygen carrier to prepare high-quality syngas, which is suitable for high-value-added downstream chemical products (Adanez et al., 2012). Therefore, the concept of CLR targets the production of H<sub>2</sub> + CO by partially oxidizing methane in the fuel reactor by the lattice oxygen of a solid oxygen carrier while the oxygen-depleted material is re-oxidized in an air reactor (Y. Sun et al., 2022). The heat generated from the redox reactions is used for the endothermic steam/dry reforming of methane to produce H<sub>2</sub> + CO (Argyris et al., 2022). The chemical looping reforming consists of two reactors, most commonly fixed beds, moving beds and fluidized beds. To choose the right reactor configuration, several factors such as target heat/mass transfer rates, reaction kinetics, and the desired extent of reduction of the oxygen carriers should be considered (Z. Sun et al., 2020). Depending on the ratio of oxygen to fuel and the nature of the oxygen carrier, the following reactions can occur during a methane reforming process that can affect the reactor design and syngas selectivity targets (Z. Sun et al., 2020).

Partial methane oxidation:



Full methane oxidation:



Methane decomposition:



Water-gas shift:



Steam methane reforming:



Dry methane reforming:



From a product selectivity point of view, various products can appear in methane reduction according to the above equations. Although Fe-based materials are attractive oxygen carriers due to environmental compatibility, low cost, and thermodynamic advantages, pure iron oxides cannot meet the requirements of methane reforming in terms of methane conversion and hydrogen selectivity (Neal et al., 2015). Therefore, Fe-based materials need to be deeply reduced to FeO/Fe to produce hydrogen. Furthermore, as the reactivity of Fe to methane is low compared with other transition metals (Guerrero-Caballero et al., 2019), many researchers have studied adding promoters to enhance the reactivity to methane. In comparison to Fe-based materials with 84% methane conversion, Fe-Ni, Fe-Co and Fe-Cu showed respectively 92%, 83% and 85% methane conversion in CLR of methane at 900 °C, indicating methane decomposition rather than methane oxidation with lattice oxygen led to high methane conversion. It was shown that the promoters have a positive effect on the hydrogen purity of iron oxygen carriers. The hydrogen purity of methane reforming after 10 cycles was reported 91%, 94%, 98% and 100% for Fe, Fe-Ni, Fe-Cu and Fe-Co, respectively. Co can increase the amount of active lattice oxygen

1  
2  
3  
4  
5  
6  
7  
8  
9  
10  
11  
12  
13  
14  
15  
16  
17  
18  
19  
20  
21  
22  
23  
24  
25  
26  
27  
28  
29  
30  
31  
32  
33  
34  
35  
36  
37  
38  
39  
40  
41  
42  
43  
44  
45  
46  
47  
48  
49  
50  
51  
52  
53  
54  
55  
56  
57  
58  
59  
60

instead of the activity of lattice oxygen, and Cu can activate the initial reduction but restrain the deep reduction of Fe-based oxygen carriers. The strongest interaction with Fe was observed in Ni-promoted oxygen carriers and a small amount of addition can increase the extend of deep reduction. Therefore, the addition of Ni, Co and Cu to Fe-based oxygen carriers can offer the higher H<sub>2</sub> purity and (H<sub>2</sub>-CO) yield but a lower CO purity due to enhanced ability to oxygen diffusion (J. Hu, Chen, et al., 2021).

Compared to the methane steam reforming reaction, the reaction rate in partial oxidation of methane was reported to be hundreds of times higher. Furthermore, it has been reported that reaction performance in methane reforming unit is relatively sensitive to temperature changes in a temperature range of 500 °C to 700 °C (Y. ke Zhang et al., 2021). (Qin et al., 2018) proved that the addition of 1% of Cu dopant to Fe-based oxygen carriers leads to a higher reactivity at low temperatures. Based on their funding, the methane conversion rate in Cu-Fe<sub>2</sub>O<sub>3</sub> is 470% higher than that Fe<sub>2</sub>O<sub>3</sub> at 700 °C which results in a decrease in energy consumption by up to 35%.

Detailed study of the effect of steam flow to oxygen carrier ratio and methane flow to oxygen carrier ratio on methane conversion and product yield in steam methane reforming was performed by several researchers (Z. Hu et al., 2021). It was reported that hydrogen concentration decreases when steam flow to oxygen carrier ratio increases while CO<sub>2</sub> and CO concentrations increased. This can be explained by the fact that that CH<sub>4</sub> complete oxidation reaction is limited under the condition of high steam concentration, which leads to the oxidation of CH<sub>4</sub> into CO<sub>2</sub> and H<sub>2</sub> and the conversion of CH<sub>4</sub> into carbon and H<sub>2</sub>. The CO<sub>2</sub> generated in the reaction process is absorbed by CaO to produce CaCO<sub>3</sub>. When steam to oxygen carrier ratio increases, the CO<sub>2</sub> concentration increases slightly. Moreover, the excessive steam promotes the oxidation of carbon to produce CO. Therefore, the H<sub>2</sub> concentration decreases and the concentration of CH<sub>4</sub> and CO increases with the increase of steam to oxygen carrier ratio.

In addition, less carbon deposition and lower methane conversion can be expected in methane reforming when steam to oxygen carrier ratio increases. The carbon deposition generated in the reaction process came from the decomposition of  $\text{CH}_4$ . When steam to oxygen carrier ratio rise,  $\text{H}_2\text{O}$  reacted with the deposited carbon to generate  $\text{CO}$  and  $\text{H}_2$ , so the carbon deposition was lower under the condition of higher steam to oxygen carrier ratio. It was observed that methane conversion and hydrogen concentration decreased as the methane flow to oxygen carrier ratio increased because in the high methane flow, oxygen carrier does not have enough active sites to react with the excessive methane, which causes a decrease in methane conversion (Z. Hu et al., 2021). In comparison to steam methane reforming and methane partial oxidation, the dry reforming of methane maintains a ratio of  $\text{H}_2/\text{CO}$  equal to 1, which enables better production of oxygenated chemicals and hydrocarbons (Usman et al., 2015). In dry reforming of methane, the ratio of  $\text{H}_2/\text{CO}$  increases and gets closer to unity as temperature increases up to  $800^\circ\text{C}$  due to the endothermic nature of the process (Hassani Rad et al., 2016). The reverse water-gas shift reaction and  $\text{CO}_2/\text{CH}_4$  ratio plays important roles in the dry reforming of methane without  $\text{O}_2$  addition. (Chein & Fung, 2019) concluded that by increasing  $\text{CO}_2/\text{CH}_4$  amount in feedstock, methane conversion increases while  $\text{H}_2$  yield decreases.

The steam to carbon ratio is an important factor in defining the methane and product distribution pathways in CLR of methane. The high concentration of steam in the process is not favored as it increases the operating costs and reduces the energy efficiency of the system. Therefore, an appropriate value of steam/carbon ratio should be considered. The changes in methane conversion, product selectivity and syngas ratio was evaluated by (Nazari et al., 2021) as illustrated in **Figure 1**.

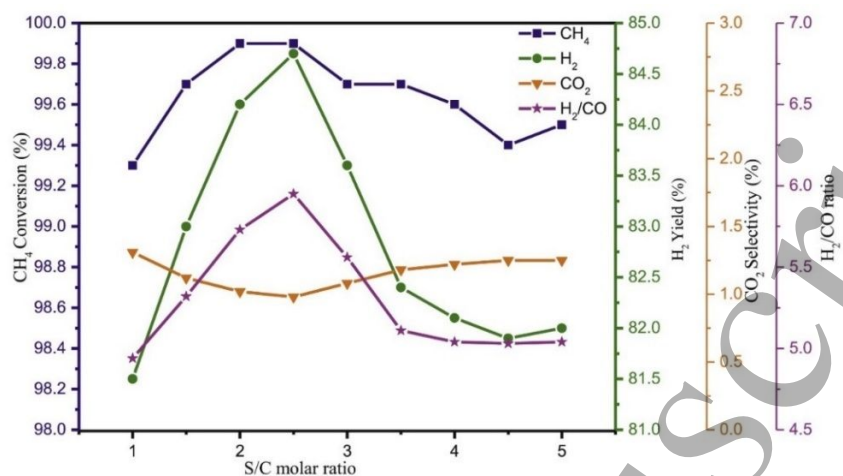


**Figure 1.** Methane conversion, hydrogen yield, CO<sub>2</sub> selectivity and H<sub>2</sub>/CO ratio at 650 °C as a function of Steam/Carbon molar ratio. Reprinted with permission from (Nazari et al., 2021). 2021, Elsevier.

The increasing the bed height over fuel reactor is beneficial for the reforming application with natural gas as fuel in a fluidized bed reactor due to an enhancement in methane conversion. This behavior can be explained by the fact that the high bed height means an increase in residence time, which is favorable to the oxidation of surface carbide from the dissociation of methane (Dai et al., 2012). Further research on impact of temperature in CLR of methane was undertaken by (Iglesias et al., 2017). It was reported that as reaction temperature increases, CO selectivity increases, owing to bulk oxygen mobility being favored in high-temperature conditions. Furthermore, the hydrogen yields, and methane conversion increased with temperature. Compared to NiO/NiAl<sub>2</sub>O<sub>4</sub>, NiO/MgAl<sub>2</sub>O<sub>4</sub> exhibit better reforming properties, higher methane conversion and higher stability against carbon formation. in a fluidized bed reactor at 950 °C (Johansson et al., 2008).

Operating pressure is another important parameter that should be taken into consideration because of its effect on product distributions in CLR. It was reported that CO<sub>2</sub> and CH<sub>4</sub> conversions decrease when pressure increases from 1 bar to 25 bar. Therefore, it is suggested to operate CO<sub>2</sub> reforming of methane at atmospheric pressure to achieve high syngas yield and conversions (Nikoo & Amin, 2011). Furthermore,

carbon deposition significantly increases with a rise in pressure. However, (Spallina et al., 2017) tested CLR in packed-bed reactors with integrated CO<sub>2</sub> capture at high pressure around 20 bar and a temperature range from 600 to 900 °C. A CH<sub>4</sub> conversion of 92% during reforming was reported with near-zero CO<sub>2</sub> emissions. They proved that the combination of chemical looping combustion and steam reforming can be accomplished through sequential heat storage and heat removal. (Argyris et al., 2022) successfully demonstrated a CLR packed bed reactor and observed that pressure is a key factor in oxidation in low-velocity operation where higher pressures produced better solid conversion.

The summary of this section is as follows:

- Pure iron oxides cannot meet the requirements of methane reforming in terms of CH<sub>4</sub> conversion and hydrogen selectivity.
- The addition of Ni, Cu and Co to iron-based oxygen carriers exhibits a positive effect on the hydrogen purity in CH<sub>4</sub> reforming processes.
- Among Ni, Fe, Mn, Cu and Co, both Ni and Cu-based oxygen carrier exhibit high reactivity whereas their selectivity toward partial oxidation of CH<sub>4</sub> for syngas production is poor; Fe and Ce based oxygen carrier possess high selectivity of CO and H<sub>2</sub> toward partial oxidation of CH<sub>4</sub>, but their reactivity is low toward CH<sub>4</sub>.
- To choose the right reactor configuration, heat transfer rates, reaction kinetics, and the desired extent of reduction of the oxygen carriers should be considered.
- By increasing temperature in fuel reactor, CO selectivity, the hydrogen yields and methane conversion increase.
- The carbon deposition increases with a rise in operating pressure.

- Increasing the bed height over fuel reactor is beneficial for the reforming application in fluidized bed reactors.
- Fluidized bed reactors can improve the methane conversion rate and syngas selectivity compared to the fixed bed reactors.

2.2 Chemical looping reforming of ethanol

Hydrogen can be produced from various types of hydrocarbon and oxygenated-hydrocarbon compounds. Although the main experience of obtaining hydrogen by the chemical looping reforming process is with gaseous fuels like methane, liquid fuels are becoming more relevant in the last years. Less hazardous, high energy density, relatively high storage safety and transportation, low cost and high availability make ethanol a renewable and carbon-neutral candidate to produce hydrogen (Saupsor et al., 2020). The hydrogen production from ethanol in the chemical looping reforming approach over  $Me_xO_y$  oxygen carrier consists of three main mechanisms as follows(Saupsor et al., 2021):

Thermal decomposition of ethanol:



Ethanol partial oxidation:



Ethanol steam reforming:



The produced CO can further react with  $H_2O$  via a water-gas shift reaction as follows:





For ethanol reforming Ni and Rh-based materials are the most studied oxygen carriers due to their high hydrogen selectivity. For example, ethanol can be fully converted into gaseous products, composed mainly of  $H_2$ ,  $CH_4$ ,  $CO$ , and  $CO_2$  over CuO-NiO material. Furthermore, the addition of Cu metal into Ni improves the hydrogen selectivity and decreases CO concentration from ethanol. (Dou et al., 2018) obtained hydrogen selectivity of 97% and ethanol conversion in a range of 82 to 93 % at 873 K over NiO/ $Al_2O_3$ . The experimental values of hydrogen production in their investigation were lower than those by equilibrium calculations, which could be due to the oxygen carrier reduction effects to consume the ethanol feeding. Although Ni shows an attractive candidate for CLR of ethanol, some researchers observed carbon deposition on the catalyst surface (Saupsor et al., 2021)

(López Ortiz et al., 2015) conducted a thermodynamic analysis and concluded that in the ethanol reforming process over NiO oxygen carrier, the maximum hydrogen content occurred in a temperature range of 625 to 679 °C. Furthermore,  $CO_2$  mols followed the same trend as  $H_2$  content, while CO and  $CH_4$  content reduced. This behavior is consistent with the promotion of the water gas shift and the steam reforming of methane reactions by increasing temperature. One of the advantages of utilizing ethanol over Ni-based materials is the absence of deactivation processes by sulphur that normally happens when fossil fuels are used. (W. Wang et al., 2017) showed that Ni-based oxygen carriers offer a better catalytic activity than Mn-based materials for the higher hydrogen yield in CLR of ethanol.

The product yield in ethanol reforming not only depending on the type of oxygen carrier but also depending on operating parameters such as temperature, water to ethanol ratio and oxygen to ethanol ratio. **Figure 2a** indicates that at 500 °C, methane exhibited its highest yield while hydrogen offered its lowest yield, which means ethanol decomposition was one of the main reactions at this temperature. When the temperature increases from 500 °C to 600 °C, the hydrogen yield increased significantly, but the methane yield decreased suddenly indicating ethanol decomposition isn't the main reaction anymore.

According to **Figure 2b**, the water/ethanol molar ratio seems to have a strong influence on hydrogen yield at 600 °C. As the water/ethanol ratio increases, H<sub>2</sub> and CO<sub>2</sub> yield increase continuously. The CO and CH<sub>4</sub> yield decrease with a rise in the molar ratio from 3 to 7. It can be concluded that methane reforming and WGS were promoted. When water/ethanol ratio increases to 7, the methane yield remains constant. (García-Labiano et al., 2015b) claimed that an increase in the oxygen to ethanol ratio reduces hydrogen concentration and increases CO<sub>2</sub> concentration over NiO/Al<sub>2</sub>O<sub>3</sub>.

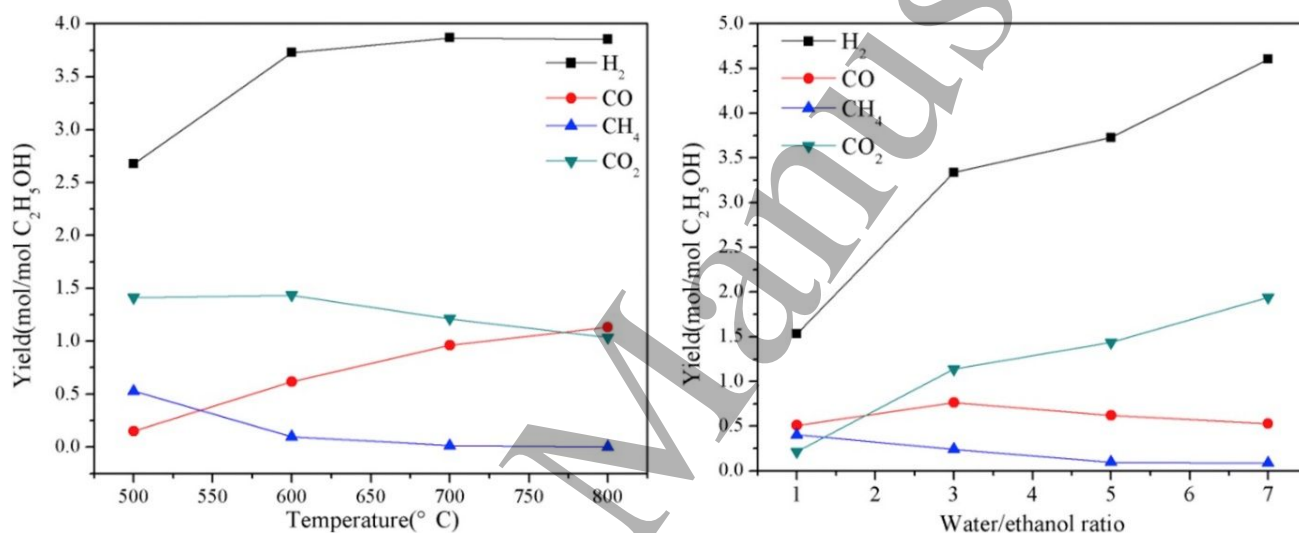


**Figure 2(a,b).** The products yield in chemical looping reforming of ethanol. Reprinted with permission from (W. Wang et al., 2017). 2016, Elsevier.

The thermodynamic investigations conducted by (Yang et al., 2011) showed that hydrogen selectivity from ethanol reforming is higher than that from glycerol reforming at 650 °C. It was also found that more water has to be consumed in glycerol reforming to achieve the same hydrogen selectivity, which causes a higher energy cost to vaporize water. It may be due to the higher O/C ratio in a glycerol molecule. The more abundance of O in the glycerol system limits the WGS and enhances the oxidation of H<sub>2</sub>, which lower the extent to extract hydrogen from water. Therefore, from the view of producing hydrogen ethanol reforming is more efficient than glycerol reforming. Furthermore, the authors concluded that glycerol

reforming is more resistant to carbon deposition as the coke is formed at lower temperatures in ethanol reforming compared to glycerol reforming as given in **Figure 3**. This can be explained by the more oxygen atoms in glycerol molecule than in ethanol, which facilitates the formation of gaseous CO or CO<sub>2</sub>.

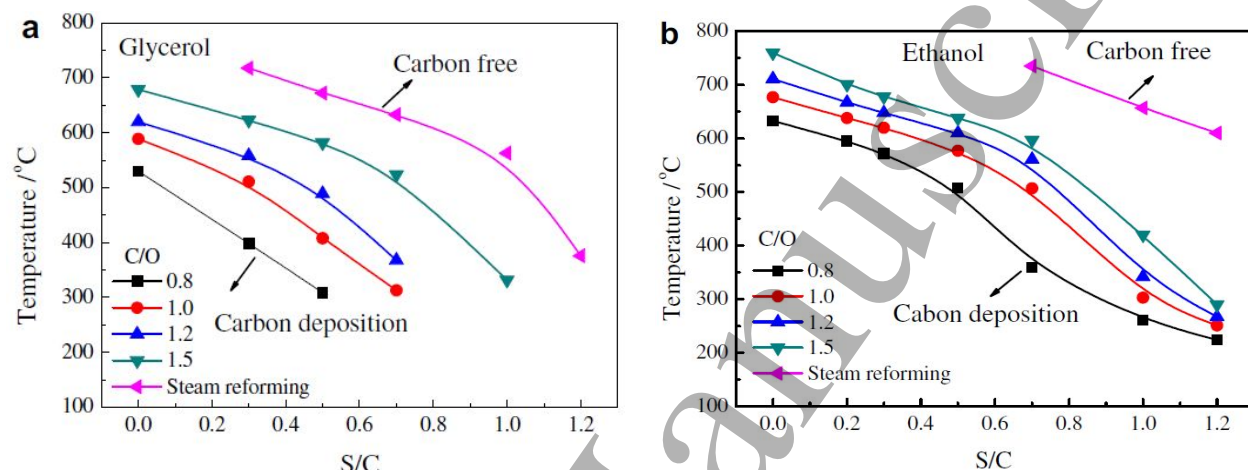


**Figure 3.** Comparison of chemical looping reforming of glycerol and ethanol. Reprinted with permission from (Yang et al., 2011). 2011, Elsevier.

The key messages of this section can be summarized as follows:

- Ni and Rh-based materials are the most common oxygen carriers in ethanol reforming due to their high hydrogen selectivity.
- The addition of Cu metal into Ni improves the hydrogen selectivity and decrease CO concentration.
- In the ethanol reforming over NiO, the maximum hydrogen content occurs in a temperature of 625 to 679 °C and at water/ethanol ratios of 6 and 3.
- The hydrogen selectivity from ethanol reforming is higher than that from glycerol reforming at 650 °C.
- An increase in the oxygen-to-ethanol molar ratio reduces hydrogen concentration and increases CO<sub>2</sub> concentration.

- Ni-based oxygen carriers offer a better catalytic activity than Mn-based materials for the higher hydrogen yield in ethanol reforming system.
- The water to ethanol molar ratio showed a strong influence on hydrogen yield.

### 2.3 Chemical looping reforming of glycerol

Biodiesel production around the world had experienced a huge increase in the last years. Glycerol, as the main by-product, is produced by the conversion of animal-based or vegetable oils into biodiesel through the catalytic trans-esterification process. Although the purification process of glycerol is expensive and complicated, crude glycerol must be purified before it can be used due to its impurities (Suero et al., 2015). To address this issue, the hydrogen production technology of glycerol steam reforming due to its good industrial application prospects has increasingly attracted increased attention in the past decades. It is noteworthy to mention that methane is a non-renewable resource, hence glycerol might be an attractive option due to its renewability. The catalyst-to-feed ratio, steam-to-carbon ratio and temperature are the most important factors in the glycerol steam reforming process while major concerns are high energy consumption, byproduct formation and catalyst deactivation (Iliuta, 2013). Steam reforming of glycerol is the most well-known and preferable technique for H<sub>2</sub> production because it can theoretically make 7 mol of H<sub>2</sub> with the consumption of 1 mol glycerol (Patcharavorachot et al., 2019) as follows:



The following side reactions also take place during glycerol steam reforming which might affect the yield and selectivity of the target product (Qingli et al., 2021). The used oxygen carriers for glycerol reforming should have the ability to break the C-C, C-H and H-O bonds and promote the water-gas shift reaction

to form hydrogen and CO<sub>2</sub> as well as it should maintain the ability of C=O bonds, which improves the selectivity of hydrogen.

Glycerol pyrolysis:



Water-gas shift reaction:



Methanation reactions



methane decomposition:



CO disproportionation reaction:



Ni-based oxygen carriers with a low cost and strong ability to break O-H, C-H and C-C bonds have been evaluated for utilization in glycerol reforming processes. A comparative study by (Adhikari et al., 2007) on glycerol conversion and product composition over various oxygen carriers in CLR of glycerol showed that the glycerol conversion can be ranked in the order Ni > Ir > Pd > Rh > Pt > Ru, while hydrogen selectivity was found to be in the order Ni > Ir > Ru > Pt > Rh > Pd. Catalytic conversion of glycerol to H<sub>2</sub>, CO<sub>2</sub>, and CO involves the preferential cleavage of C–C bonds as opposed to C–O bonds. It is generally accepted that nickel promotes C–C rupture.

The effect of operating variables such as O<sub>NiO</sub>/glycerol and H<sub>2</sub>O/glycerol on the synthesis composition needs to be examined since in CLR process, water addition is utilized to improve hydrogen production as well as to minimize carbon deposition. **Figure 4** shows that higher values of H<sub>2</sub> and CO can be

1  
2  
3  
4  
5  
6  
7  
8  
9  
10  
11  
12  
13  
14  
15  
16  
17  
18  
19  
20  
21  
22  
23  
24  
25  
26  
27  
28  
29  
30  
31  
32  
33  
34  
35  
36  
37  
38  
39  
40  
41  
42  
43  
44  
45  
46  
47  
48  
49  
50  
51  
52  
53  
54  
55  
56  
57  
58  
59  
60

obtained at a lower  $O_{NiO}/\text{glycerol}$  ratio due to the higher contribution of the partial oxidation with respect to the glycerol combustion because of the lower lattice oxygen availability. As given in **Figure 5**,  $H_2/CO$  ratio is a strong function of water amount in feedstock. At all temperatures,  $H_2/CO$  ratio and  $CO_2$  concentration increase with a rise in  $H_2O/\text{glycerol}$  ratio from 0.25 to 2 due to the enhancement of the direct glycerol reforming and the water-gas shift reaction. It is evident that the  $H_2/CO$  ratio decreases from 2.15 to 1.35 when fuel reactor temperature increases from 750 to 850 °C due to the increase in the CO formation while the  $H_2$  remained almost constant with the temperature.

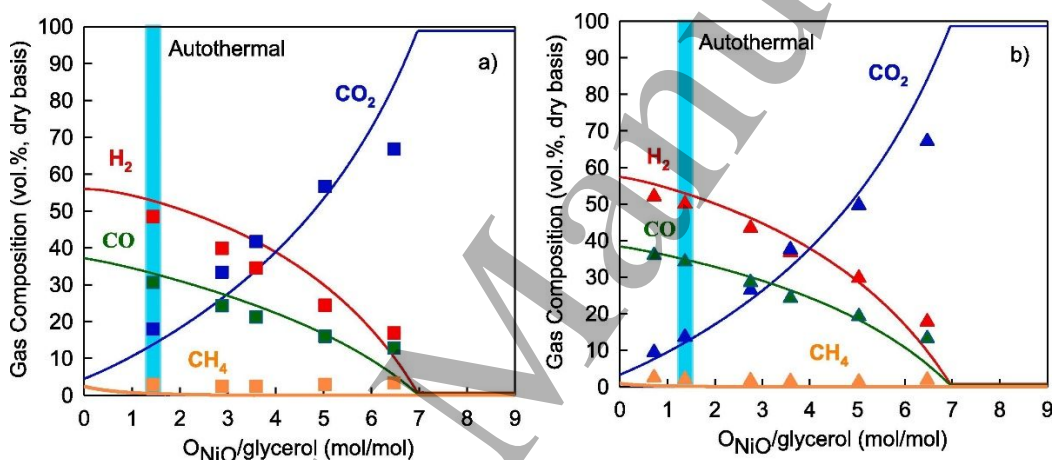


**Figure 4.** Effect of  $O_{NiO}/\text{glycerol}$  ratio in the composition of the fuel reactor gas stream at a) 750 °C; b) 800 °C.

Reprinted with permission from (Adánez-Rubio et al., 2021). 2020, Elsevier.

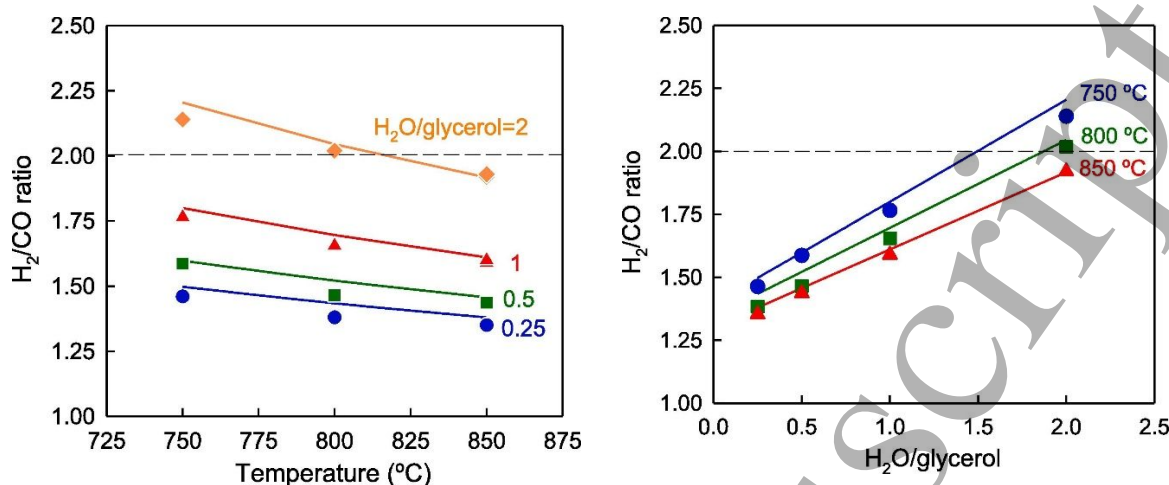


**Figure 5.**  $H_2/CO$  ratio as a function of the fuel reactor temperature and  $H_2O/glycerol$  in glycerol reforming.

Reprinted with permission from (Adánez-Rubio et al., 2021). 2021, Elsevier.

(Delparish et al., 2019) showed full conversion of glycerol can be determined at steam to carbon ratio equal to 5, C/O range of 0.75 to 1.25, and at temperatures from 550 to 700  $^{\circ}C$ . Their findings indicated that yields of  $H_2$  and  $CO_2$  increase with the increasing amount of steam in the feed while CO yield decreases. It can be explained by the fact that the WGS reaction is favored at higher amounts of inlet steam to transform CO into  $H_2$  and  $CO_2$ .

One of the main parameters in the liquid reforming by chemical looping reforming technique is oxygen-to-fuel molar ratio as the amount of lattice oxygen transferred by the oxygen carrier in the fuel reactor controls the reforming process and product composition. To achieve lower  $H_2/CO$  ratio suitable in downstream, researchers added  $CO_2$  to feedstock in steam CLR of glycerol (Tavanarad et al., 2021). Feeding glycerol with  $CO_2$  to fuel reactor decreases  $H_2/CO$  ratio which can be attributed to the positive effect of the excess  $CO_2$  on the reverse water-gas shift reaction. The glycerol conversion shows higher values at a higher  $CO_2/glycerol$  molar ratio.

From an economic point of view, it is not desirable to heat and pump more water through the system than is necessary. An increase at concentration of glycerol in feed has a positive effect on  $H_2$  yield while

decreases CH<sub>4</sub> yield, (Byrd et al., 2008). This can be explained by the fact that at low steam/carbon ratios (high glycerol concentration) CO is more likely to produce methane by consuming hydrogen.

Gas hourly space velocity has a significant effect on glycerol conversion and product composition in glycerol reforming. It was observed that glycerol conversion increases when gas hourly space velocity decreases. The residence time of reactants decreases and the pressure drop of the reactor increases at higher gas hourly space velocity which leads to higher coke formation over the catalysts surface and less glycerol conversion. Based on the results above, the yield of H<sub>2</sub> production in CLR of glycerol depends on oxygen carrier follows the order CuO (81.00%) < NiO (81.07%) < CoO (81.14%) < Co<sub>3</sub>O<sub>4</sub> (81.80%) < Fe<sub>2</sub>O<sub>3</sub> (83.66%) < Mn<sub>2</sub>O<sub>3</sub> (87.33%) < Mn<sub>3</sub>O<sub>4</sub> (87.54%) indicating Mn-based materials have great potential in CLR of glycerol applications.

The important conclusions of this section are as follows:

- The most important parameters in the glycerol steam reforming process are temperature, steam-to-carbon ratio, and catalyst-to-feed ratio.
- Major concerns in glycerol reforming are by-product formation, catalyst deactivation, and high energy consumption.
- The glycerol conversion over various oxygen carriers can be ranked in the following: Ni > Ir > Pd > Rh > Pt > Ru.
- The gas hourly space velocity has a significant effect on glycerol conversion and product composition in glycerol reforming.
- The yield of H<sub>2</sub> production in glycerol reforming over various oxygen carriers is in accordance with the order of CuO < NiO < CoO < Co<sub>3</sub>O<sub>4</sub> < Fe<sub>2</sub>O<sub>3</sub> < Mn<sub>2</sub>O<sub>3</sub> < Mn<sub>3</sub>O<sub>4</sub>.
- H<sub>2</sub>/CO ratio in glycerol reforming is a strong function of water amount in feedstock.



### 3. Recent advances in oxygen carriers for CLR

The solid oxygen carrier materials that are used in chemical looping technologies to transfer oxygen from the air to the fuel have a key role in the success of the process for the production of hydrogen (J. Hu, Zhang, et al., 2021). In this regard, extensive research has been made toward the development of optimum oxygen carrier materials with improved properties which will be discussed in this section. The oxygen carriers can be divided into two main categories including synthetic materials and natural minerals. Although natural minerals are cheap, their reactivity is usually lower than synthetic oxygen carriers (Adanez et al., 2012). Metal oxides of Fe, Ni, Co and Mn with inert support such as  $\text{TiO}_2$ ,  $\text{Al}_2\text{O}_3$  and  $\text{SiO}_2$  are the most studied synthetic oxygen carriers in the literature which possess their individual advantages and weaknesses. As chemical looping processes are often operate at high temperatures in industrial application, it is critical to select a suitable oxygen carrier based on its thermal stability to avoid material sintering. The melting temperature of several different transition-state metals and their corresponding oxides have been listed in **Table 3**. In addition, the maximum oxygen transport capacity of oxygen carriers was also given in this table. Oxygen carriers with a low circulation rate are suitable from design simplicity and less circulation power point of view. However, it should be high enough to transport sufficient oxygen for complete fuel oxidation as well as to transport the desired heat in case of an endothermic reaction in the fuel reactor (Abuelgasim et al., 2021).

To ensure the oxygen carriers have desirable qualities, an understanding of the reaction mechanism and morphological changes during the reaction are needed. The various competing factors such as resistance to toxicity, easy scalability, complete fuel conversion to CO and  $\text{H}_2$ , environmental aspects, low cost, availability, high attrition resistance, high conversion rate, and stability under repeated oxidation/reduction, high oxygen-carrying capacity and good heat-carrying capacity should take into

account before selection of an appropriate oxygen carrier (Z. Sun et al., 2020). However, it is not easy to find a metal oxide that could meet all the above factors. In this regard, supporting materials such as  $\text{MgAl}_2\text{O}_4$ ,  $\text{ZrO}_2$ ,  $\text{SiO}_2$ ,  $\text{TiO}_2$  and  $\text{Al}_2\text{O}_3$  can be added to metal oxides to improve attrition resistance and mechanical strength. Furthermore, depending on which preparation method is used for oxygen carriers, their properties can change. There are several methods to prepare oxygen carriers including spray pyrolysis, sol-gel, spray drying, pelletizing by extrusion, precipitation, mechanical mixing, impregnation, hydrothermal synthesis, dissolution, freeze granulation, deposition precipitation, co-precipitation and citric acid method (Long et al., 2020) (T. Li et al., 2020) (Rydén et al., 2011). Many materials have been investigated in the literature for the chemical looping operation and are presented in the following sections. A summary of different kinds of oxygen carries utilized in chemical looping processes was also listed in **Table 4**.

**Table 3:** Melting temperature and maximum oxygen transport capacity of most common oxygen carriers.

Data taken from (Adanez et al., 2012) (Jerndal et al., 2006)(Adánez et al., 2018)

Oxidation/reduction form	Melting temperature (°C)	Maximum oxygen transport capacity
NiO / Ni	1955 / 1455	0.214
CuO / Cu	1446 / 1085	0.201
CuO / Cu <sub>2</sub> O	1446 / 1235	0.101
FeO / Fe	1377 / 1538	0.222
Fe <sub>2</sub> O <sub>3</sub> / Fe <sub>3</sub> O <sub>4</sub>	1565 / 1597	0.034
Fe <sub>2</sub> O <sub>3</sub> / Fe	1565 / 1538	0.100
Mn <sub>3</sub> O <sub>4</sub> / MnO	1562 / 1842	0.070
Mn <sub>2</sub> O <sub>3</sub> / Mn <sub>3</sub> O <sub>4</sub>	1347 / 1562	0.034
CoO / Co	1830 / 1495	0.214
Co <sub>3</sub> O <sub>4</sub> / CoO	1830 / 1830	0.067
Ce <sub>2</sub> O <sub>3</sub> / CeO <sub>2</sub>	2230 / 2400	0.048
BaSO <sub>4</sub> / BaS	1580 / 2230	0.274
SrSO <sub>4</sub> / SrS	1607 / 2227	0.348

**Table 4:** Summary of the oxygen carriers tested in different chemical looping reforming units

Metal carrier	Support material	Synthesis method	Ref.
---------------	------------------	------------------	------

Fe, Mn, Co, Cu	Al <sub>2</sub> O <sub>3</sub>	Co-precipitation	(Forutan et al., 2015)
Fe, Ni, Mn	Al <sub>2</sub> O <sub>4</sub>	Impregnation	(Svoboda et al., 2008)
Fe	Al <sub>2</sub> O <sub>4</sub>	Commercial	(Lu et al., 2021)
Cu	Al <sub>2</sub> O <sub>4</sub>	Commercial	(L. Guo et al., 2015)
Cu	Al <sub>2</sub> O <sub>3</sub>	Incipient wetness impregnation	(Keller et al., 2016)
Cu	Al <sub>2</sub> O <sub>3</sub>	Co-precipitation	(Alirezai et al., 2016)
Ni	γAl <sub>2</sub> O <sub>3</sub>	Impregnation	(Rydén et al., 2008)
Ni	αAl <sub>2</sub> O <sub>3</sub>	Incipient wetness impregnation	(Garcia-Labiano et al., 2014)
Ni	Al <sub>2</sub> O <sub>3</sub>	Commercial	(Yahom et al., 2014)
Fe-Cu	Al <sub>2</sub> O <sub>3</sub>	Commercial	(Sirwardane et al., 2015)
Fe, Ni, Co	CeO <sub>2</sub>	Impregnation, Co-precipitation	(Guerrero-Caballero et al., 2019)
Fe-Ni	Al <sub>2</sub> O <sub>3</sub>	Co-precipitation	(G. Wei et al., 2019)
Fe	Al <sub>2</sub> O <sub>3</sub>	sol-gel synthesis	(Solunke & Vesper, 2010)
CeO <sub>2</sub>	γAl <sub>2</sub> O <sub>3</sub>	Incipient wetness impregnation	(Y. Wei et al., 2007)
Ni-Cu	Al <sub>2</sub> O <sub>3</sub>	Hydrothermal syntheses	(J. Huang et al., 2019)
Co	CeO <sub>2</sub>	Wet-impregnation	(Ayodele et al., 2016)
Cu	γAl <sub>2</sub> O <sub>3</sub>	Incipient wet impregnation	(Forero et al., 2011)
Ni-CeO <sub>2</sub>	Al <sub>2</sub> O <sub>3</sub>	Co-precipitation	(Rahbar Shamskar et al., 2017)
Ni-CeO <sub>2</sub>	Al <sub>2</sub> O <sub>3</sub>	Incipient wetness impregnation	(Chein & Fung, 2019)
Ni-Ce	MgO	Impregnation	(Khajenoori et al., 2015)
Ni	SiO <sub>2</sub> , Al <sub>2</sub> O <sub>3</sub>	Incipient wetness impregnation	(Nieva et al., 2014)
Ni, Co, Cu	SiO <sub>2</sub>	Incipient wetness impregnation	(Papageridis et al., n.d.)
Ni, Co, Cu	γAl <sub>2</sub> O <sub>3</sub>	Incipient wetness impregnation	(Papageridis et al., 2016)
Co	Al <sub>2</sub> O <sub>3</sub>	Commercial	(Jerndal et al., 2006)
CuO	TiO <sub>2</sub>	self-assembly combustion synthesis	(Tian et al., 2020)
CuO	ZrO <sub>2</sub>	Incipient wetness impregnation	(Adánez-Rubio et al., 2020)
Fe <sub>2</sub> O <sub>3</sub>	Al <sub>2</sub> O <sub>3</sub>	sol-gel synthesis	(Y. Kang et al., 2019)
CeO <sub>2</sub>	Fe <sub>2</sub> O <sub>3</sub>	Chemical precipitation	(X. Zhu et al., 2014)
Fe <sub>2</sub> O <sub>3</sub> /CeO <sub>2</sub>	ZrO <sub>2</sub>	Co-precipitation	(Yamaguchi et al., 2011)
CeO <sub>2</sub>	ZrO <sub>2</sub>	Precipitation	(Jang et al., 2014)
NiO, CuO, Fe <sub>2</sub> O <sub>3</sub>	SiO <sub>2</sub>	dry impregnation	(Zafar et al., 2005)
NiO	ZrO <sub>2</sub> , TiO <sub>2</sub> , SiO <sub>2</sub>	dry impregnation	(Antzara et al., 2016)
Cu-Fe	Al <sub>2</sub> O <sub>4</sub>	Co-precipitation	(Imtiaz et al., 2015)
Ni-Fe	Al <sub>2</sub> O <sub>4</sub>	Co-precipitation	(J. Huang et al., 2018)
Cu-Ni	Al <sub>2</sub> O <sub>3</sub>	Impregnation	(Khzouz et al., 2013)
Cu-Fe	Al <sub>2</sub> O <sub>3</sub>	Impregnation, Co-precipitation	(Chiron & Patience, 2012)
Cu	Al <sub>2</sub> O <sub>3</sub>	Wet-impregnation	(X. Zheng et al., 2014)
CeO <sub>2</sub>	N.A.	Precipitation	(X. Zhu et al., 2011)
Ni	CeO <sub>2</sub> , La <sub>2</sub> O <sub>3</sub>	Co-precipitation, Impregnation	(Pantaleo et al., 2015)

Ce <sub>x</sub> Fe <sub>10-x</sub> O	N.A.	citric acid sol-gel method	(Yan et al., 2018)
Fe-Ni	CeO <sub>2</sub>	Impregnation	(Luo et al., 2022)
CeO <sub>2</sub>	BF <sub>3</sub>	Chemical co-precipitation	(Cheng et al., 2021)
NiO	CeZrO <sub>4</sub>	Impregnation	(Y. ke Zhang et al., 2021)
Ni, Co, Cu, Fe	MgAl <sub>2</sub> O <sub>4</sub>	Co-precipitation	(J. Hu, Chen, et al., 2021)
Ni-Fe	Calcite	Wet-impregnation	(Z. Hu et al., 2021)
Fe-CeO <sub>2</sub>	N.A.	Sol-gel Pechini method	(García-García & Metcalfe, 2021)
Ni	γAl <sub>2</sub> O <sub>3</sub>	Impregnation	(Tavanarad et al., 2021)
Ni-Mg	ATP	Impregnation	(Qingli et al., 2021)
NiO	Al <sub>2</sub> O <sub>3</sub>	Co-precipitation	(Dou et al., 2017)
Fe <sub>2</sub> O <sub>3</sub>	Al <sub>2</sub> O <sub>3</sub>	Mechanical mixing method	(Ma et al., 2020)
Ni	CeO <sub>2</sub>	Co-precipitation	(Han et al., 2022)
Co	Mg <sub>3</sub> Al	Calcination	(D. Li et al., 2018)
CeO <sub>2</sub>	LaFeO <sub>3</sub>	gas-bubble-assisted method	(Y. Zheng et al., 2017)
Mn <sub>3</sub> O <sub>4</sub>	MgZrO <sub>3</sub>	N.A.	(Lind et al., 2012)
Fe <sub>3</sub> O <sub>4</sub>	Al <sub>2</sub> O <sub>3</sub>	Commercial	(Abdalazeez et al., 2021)
Mn	ZrO <sub>2</sub>	Co-precipitation	(Alirezaei et al., 2018b)
CeO <sub>2</sub> -CuO	ZrO <sub>2</sub>	Sol-gel method	(Y. Wang et al., 2019)
Co-Fe <sub>2</sub> O <sub>3</sub>	N.A.	Sol-gel method	(M. Guo et al., 2020)
Ce-Ni	PSNT	alkalinity-tuned hydrothermal	(Jiang, Li, Bian, Li, Othman, et al., 2018)
Ni-Fe <sub>2</sub> O <sub>3</sub>	Al <sub>2</sub> O <sub>3</sub>	Impregnation	(D. Kang et al., 2018)
Ba-Co	CeO <sub>2</sub>	Sol-gel method	(Ding et al., 2019)
<b>Ni-Fe</b>	N.A.	Co-precipitation	(Z. Huang et al., 2016)
CuO-NiO	Al <sub>2</sub> O <sub>3</sub>	hydrothermal method	(Z. Wang et al., 2018)
CuO, Fe <sub>2</sub> O <sub>3</sub>	Al <sub>2</sub> O <sub>3</sub>	Sol-gel method	(H. Zhao et al., 2015)
Fe <sub>2</sub> O <sub>3</sub>	MgAl <sub>2</sub> O <sub>4</sub>	Co-precipitation	(Hafizi et al., 2016)
CeO <sub>2</sub>	ZrO <sub>2</sub>	Co-precipitation	(Y. Zheng et al., 2016)
Fe <sub>2</sub> O <sub>3</sub>	Al <sub>2</sub> O <sub>3</sub>	Co-precipitation	(M. Zhu et al., 2019)
Ni	Mn <sub>2</sub> O <sub>4</sub>	Sol-gel method	(W. Wang et al., 2017)
Cu-Fe	Al <sub>2</sub> O <sub>3</sub>	N.A.	(Nadgouda et al., 2019)
Ni-CeO <sub>2</sub>	Al <sub>2</sub> O <sub>3</sub>	Wet-impregnation	(Isarapakdeetham et al., 2020)
Ce-Fe	MgAl	Co-precipitation	(Yuan et al., 2020)
Ni-Cu/Fe <sub>2</sub> O <sub>4</sub>	N.A.	Sol-gel method	(J. Chen et al., 2019)

### 3.1. Ni-based oxygen carriers

Using nickel-based oxygen carriers for chemical looping concepts has attracted considerable attention from many researchers due to their low cost, high catalytic activity, outstanding oxygen transfer capacity

(0.21 g O<sub>2</sub>/g NiO) and great thermal stability (Roslan et al., 2020). The excellent catalytic activity of Ni has been associated with its remarkable ability for breaking the C-C bonds. Ni-based oxygen carriers were the first materials employed for demonstrating the viability of chemical looping as a carbon capture technology. The presence of nickel helps to promote the water-gas shift reaction, leading to an increase in hydrogen production. Nevertheless, they suffer from several limitations such as toxicity and coke formation on the catalyst surface, leading to blockage of nickel active sites and deactivation. A comparison between the reactivity of NiO, Mn<sub>2</sub>O<sub>3</sub>, Fe<sub>2</sub>O<sub>3</sub> and CuO metal oxides showed that the reactivity of NiO with methane is the highest while Fe<sub>2</sub>O<sub>3</sub> offer the lowest reactivity followed by CuO (Zafar et al., 2005). In addition, NiO/SiO<sub>2</sub> exhibit the highest selectivity toward hydrogen production compared to others. The reason for the low reaction rate of CuO/SiO<sub>2</sub> is the decomposition of CuO to Cu<sub>2</sub>O during the inert period following the oxidation, which means that less oxygen is available for the oxidation of the fuel. It was reported that the implementation of CO<sub>2</sub> sorption in CLR can increase the purity of hydrogen by more than 90% and decrease the operating temperature, resulting in an improvement in the stability of the Ni. The performance of Ni-based material depends significantly on metal supports that are used in catalyst preparation. It was shown that a high activity can be determined using MgAl<sub>2</sub>O<sub>4</sub> as metal support. Metal supports of SiO<sub>2</sub> and Al<sub>2</sub>O<sub>3</sub> are better candidates in terms of high temperature stability (Nieva et al., 2014).

In CLR processes, material deactivation caused by carbon deposition is one of the main issues. The several techniques such as using dry impregnation method to prepare catalyst, the addition of a small amount of alkali metals (K, Mg, Ca), type of support and the addition of a small amount of steam to the reactor were proposed in the literature to reduce carbon deposition on the material surface (Elias et al., 2013). For example, it was found that ceria-supported catalyst exhibits the lower carbon deposition

1  
2  
3  
4  
5  
6  
7  
8  
9  
10  
11  
12  
13  
14  
15  
16  
17  
18  
19  
20  
21  
22  
23  
24  
25  
26  
27  
28  
29  
30  
31  
32  
33  
34  
35  
36  
37  
38  
39  
40  
41  
42  
43  
44  
45  
46  
47  
48  
49  
50  
51  
52  
53  
54  
55  
56  
57  
58  
59  
60

compared to MgO, TiO<sub>2</sub>. Ceria establishes a better interaction with the Ni active phase, which causes a higher metal dispersion and inherently available surface area.

(Tavanarad et al., 2021) employed 15 wt% Ni supported on Al<sub>2</sub>O<sub>3</sub> with 3wt% promoters such as MgO, CaO, SrO, and BaO in the glycerol reforming. **Figure 6** shows glycerol conversion of Ni catalysts at a temperature range from 600 to 750 °C with and without promoters. As can be seen from the figure, all promoters increased the glycerol conversion and among them, SrO exhibited the highest glycerol conversion. The authors explained that this improvement could be related to the adsorption of CO<sub>2</sub> on the catalysts and the smaller crystallite sizes of the promoted catalysts. Furthermore, higher glycerol conversion on the promoted catalysts can be attributed to the enhanced basic properties of the catalysts. The addition of alkaline earth metal oxide promoters improves the adsorption of CO<sub>2</sub> on the catalysts and inhibits the Boudouard reaction, and suppresses the coke formation. The temperature showed a significant effect on glycerol conversion as it increases when temperature increases from 600 to 750 °C due to endothermic nature of the reaction.

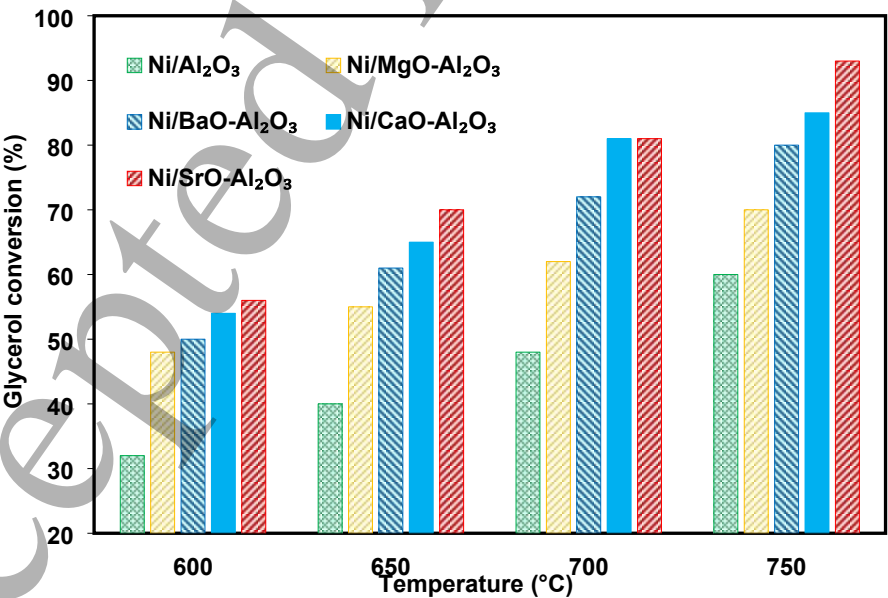


**Figure 6.** The glycerol conversion of the 15wt% Ni catalyst as a function of temperature and different promoters. Reprinted with permission from (Tavanarad et al., 2021). 2021, Elsevier.

### 3.2. Fe-based oxygen carriers

The environment friendliness, low price and good redox properties make iron-based oxygen carriers an attractive candidate for the chemical looping process (Lu et al., 2021). Furthermore, iron-based materials exhibit high melting points, and high mechanical strength and have no tendency for carbon formation or sulphide/sulphate formation. Although they offer acceptable reactivity for hydrogen and carbon monoxide, they have weak reactivity for methane (Yu et al., 2019). Similar to other oxygen carriers, iron-based materials also have a few drawbacks including low oxygen transport capacity and the complexity of heat management due to their endothermic nature (D. Li, Xu, et al., 2019). Moreover, ash compositions could react with an iron oxygen carrier which results in sintering and agglomeration (Bao et al., 2014). Generally, iron-based oxygen carriers are composed of primary iron oxide for lattice oxygen storage and ceramic support for improved redox stability and activity.

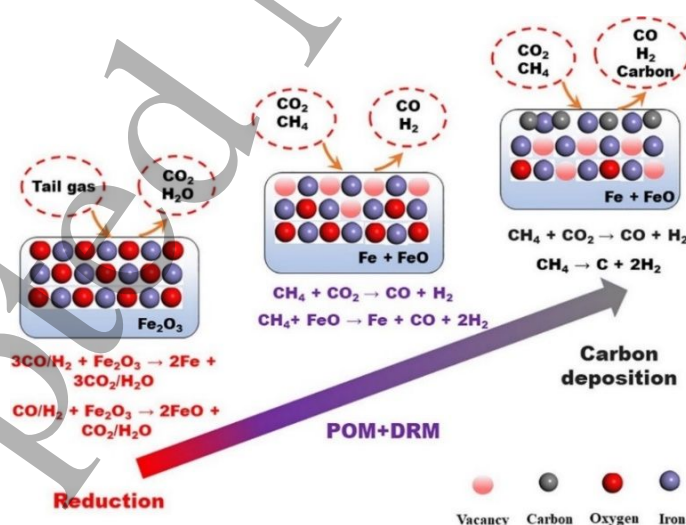


**Figure 7.** The evolution of iron oxide during the reduction and dry reforming stages. Reprinted with permission from (M. Zhu et al., 2019). 2019, Elsevier.

Evolution of iron oxide during reforming and reduction was given in **Figure 7**. During the reduction step,  $\text{Fe}_2\text{O}_3$  is reduced by gaseous fuel in order to desorb oxygen for  $\text{CO}_2$  formation and obtain adequate active sites for catalytic dry reforming of methane. In the dry reforming step,  $\text{CH}_4$  and  $\text{CO}_2$  gases are fed and the catalyst reaction of dry reforming (DRM) and partial oxidation of methane (POM) occur on the active site for syngas production along with oxygen migration. Iron-based oxygen carriers exhibit the maximum capacity for oxygen adsorption and the highest resistance against sintering compared to Co, Cu and Mn-based oxygen carriers. The optimum temperature of cobalt, magnesium, copper and iron metal oxides supported on alumina are 1298 K, 1073 K, 1303 K and 1173 K, respectively (Forutan et al., 2015). (Lu et al., 2021) studied the behavior of magnetite with  $\text{Fe}_3\text{O}_4$  in reforming of methane and observed that the temperature rise is beneficial to the reduction of iron oxide in the fuel reactor. (Guerrero-Caballero et al., 2019) performed a comparative study on several ceria-based oxygen carriers such as Ni, Co and Fe in reforming of methane. It was found that at a temperature around 873 K, Co/ $\text{CeO}_2$  shows promising results while Fe-based oxygen carrier exhibits better performance at higher temperatures. Therefore, iron-based material might be a better candidate than nickel in terms of toxicity and environmental reasons. (Solunke & Vaser, 2010) claimed that iron metal oxide is the best option from a melting point, cost, toxicity and reduction cycle point of view. The deactivation of iron oxide over multiple redox cycles is one of their limitations which leads to a decrease in CO selectivity. Moreover, the formation of  $\text{CO}_2$  during the reduction of  $\text{Fe}_2\text{O}_3$  to  $\text{Fe}_3\text{O}_4$  leads to a decrease in CO selectivity and the productivity of value-added fuels generated. The combination Fe and Ce has been suggested by several researchers due to positive effect of the addition of Ce (García-García & Metcalfe, 2021). It was reported that Fe-Ce mixed oxides produce pure hydrogen and high-quality syngas due to a strong



interaction between  $\text{CeO}_2$  and  $\text{Fe}_2\text{O}_3$  species which greatly enhances the mobility of oxygen in the Ce-Fe and improves the oxygen vacancies through the formation of  $\text{CeFeO}_3$  phases. Furthermore, the addition of  $\text{CeO}_2$  to Fe oxide leads to higher hydrogen and CO yields due to synergetic interaction between both cerium and iron oxides and the formation of a peruskite type oxide. Therefore, by controlling the amount of metal oxide in the mixture, product selectivity can be adjusted.

### 3.3. Cu-based oxygen carriers

Cu-based oxygen carriers with attractive properties have been widely studied in the literature. Great oxygen transport capacity, low toxicity, high reactivity in both reduction and oxidation cycles as well as moderate cost make Cu-based materials one of the most known oxygen carriers in chemical looping processes (Abad et al., 2007). One of the interesting advantages of this type of material is that reduction and oxidation reactions are exothermic which results in no heat supply energy requirement in the reduction reactor. Furthermore, sulphurous impurities in the fuel do not significantly affect the properties of Cu oxygen carriers (Forero et al., 2010). However, the main issue with Cu-based material is their relatively low melting point which results in agglomeration problems.

Agglomeration of oxygen carriers usually occurs when particles of oxygen carriers adhere to one another and form clusters which results in a reduction in material stability and reaction rate. To make Cu-based material a more attractive oxygen carrier, it is essential to improve its performance at high temperatures. This can be achieved using different preparation methods and addition inert supports.

For example, the efficiency of Cu oxygen carriers can be improved by the addition of 20% zirconium oxide. The 15Cu/20Zr-Al showed the highest catalytic activity with 99.2% methane conversion at 923 K. Moreover, it was found that the Zr content in the support structure could affect the coke deposition on the Cu-based oxygen carrier surface. The volumetric percentage of CO and  $\text{CO}_2$  in the reactor effluent could be related to the content of coke deposited on the oxygen carrier surface. The presence of CO and

CO<sub>2</sub> in the oxidation section is related to the burning of coke in the oxidation period. By increasing the Zr loading weight percentage, the emission of CO and CO<sub>2</sub> is decreased. The emitted CO<sub>2</sub> is reduced from about 47% to 3% by increasing the zirconium loading from 0 to 20% in the oxygen carrier support structure. Further increase in the Zr loading tends to increase the CO<sub>2</sub> percentage (Alirezaei et al., 2016). The dry impregnation of porous supports may be a better production technique compared to spray drying for chemical looping reforming bed materials due to good dispersion of the active Cu phase.

Although using CuO at high temperatures was always rejected in the literature, it was observed that an increase in the oxidation temperature up to 1173 K is feasible with CuO without any deactivation or agglomeration of the particles (Forero et al., 2011). The addition of Fe to Cu was proposed to improve material mechanical stability while maintaining a high reactivity in oxidation as well as reduction. Furthermore, combining CuO with Fe<sub>2</sub>O<sub>3</sub> can limit the temperature drop in the fuel reactor as CuO releases heat and Fe<sub>2</sub>O<sub>3</sub> reacts endothermic (Chiron & Patience, 2012).

### 3.4. Ce-based oxygen carriers

In the dry reforming of methane process, good resistance to coke is critical for catalysts and favorable from an economic point of view. Ceria-based catalysts exhibit high resistance to coke formation and have unique redox properties. Thanks to its great redox capacity, ceria is the most interesting oxide in the chemical looping partial oxidation of methane (D. Li, Li, et al., 2019). Furthermore, CeO<sub>2</sub> is very attractive in chemical looping due to the formation of Ce<sup>3+</sup> sites and CeO<sub>2</sub> oxygen vacancies, which improves the performance of various reactions. (Jang et al., 2014) used ZrO<sub>2</sub> as support for CeO<sub>2</sub> and indicated an improvement in temperature stability, redox performance and oxygen storage capacity. The production of syngas and hydrogen on CeO<sub>2</sub>-ZrO<sub>2</sub> was found to be about twice that of pure CeO<sub>2</sub> and not race of carbon deposition was observed.

(Y. Zheng et al., 2017) used  $\text{LaFeO}_3$ -supported  $\text{CeO}_2$  as an oxygen carrier and their results revealed that the presence of  $\text{CeO}_2$  improves the resistance toward carbon deposition formation, and this allows the oxygen carrier own high available oxygen storage capacity. As shown in **Figure 8**, pure  $\text{LaFeO}_3$  exhibits  $\text{H}_2/\text{CO}$  ratio of around 2.4 in the produced syngas while  $\text{CeO}_2/\text{LaFeO}_3$  showed  $\text{H}_2/\text{CO}$  ratio near 2 meaning the formation of carbon deposition in  $\text{CeO}_2/\text{LaFeO}_3$  is avoided. Since the stoichiometric reaction of a  $\text{CH}_4$  molecule with oxygen should yield a  $\text{H}_2/\text{CO}$  ratio of 2.0, ratios higher than 2 indicates the decomposition of  $\text{CH}_4$  which would result in the formation of carbon deposition. Furthermore, CO selectivity for  $\text{LaFeO}_3$  and 10% $\text{CeO}_2/\text{LaFeO}_3$  materials was also reported to be about 90% during the 30 redox cycles at 800 °C. Syngas yield for 10% $\text{CeO}_2/\text{LaFeO}_3$  ( $9.72 \text{ mmol g}^{-1}$ ) was found to be much higher than that over the pure  $\text{LaFeO}_3$  ( $5.86 \text{ mmol g}^{-1}$ ) and it is very stable during the redox testing.

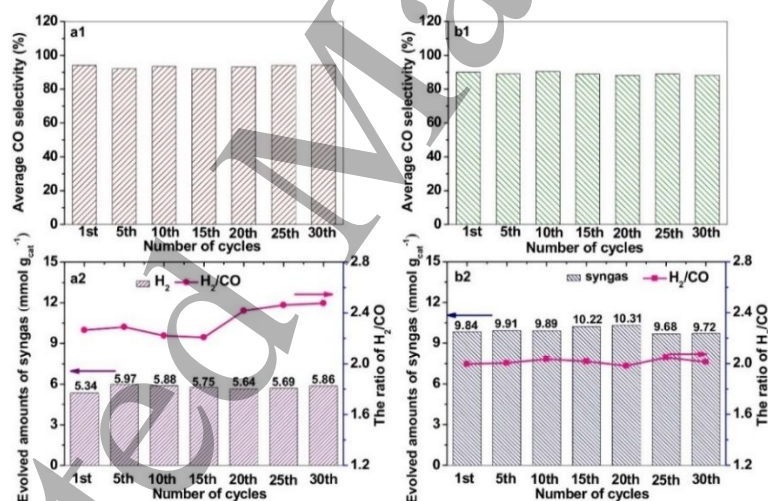


**Figure 8.** CO selectivity and syngas yield during the chemical looping reforming of methane over  $\text{LaFeO}_3$  (a1, a2) and 10% $\text{CeO}_2/\text{LaFeO}_3$  (b1, b2). Reprinted with permission from (Y. Zheng et al., 2017). 2016, Elsevier.

### 3.5. Mn-based oxygen carries

From a reactivity, cost, temperature stability and environment point of view, manganese oxide seems a potential oxygen carrier (Nandy et al., 2016). Although manganese presents a low oxygen transport capacity, their oxygen transport capacity is still greater than Fe-based materials. Mn,  $\text{MnO}$ ,  $\text{MnO}_2$ ,  $\text{Mn}_2\text{O}_3$

and  $\text{Mn}_3\text{O}_4$  are oxidation states of Mn-based oxygen carriers. Among them,  $\text{Mn}_3\text{O}_4$  is the only Mn species that shows its presence at temperatures higher than 1073 K.  $\text{Mn}_2\text{O}_3$  is thermodynamically stable in air at temperatures lower than 1173 K and  $\text{MnO}_2$  is the highest oxidation state of Mn which can be used as an oxygen carrier, tends to start decomposition in the air at about 773 K (Johansson et al., 2006). To date, few studies about using Mn-based materials can be found in the literature. (Alirezaei et al., 2018b) prepared a manganese-based oxygen carrier on  $\text{ZrO}_2$  support and applied it to production of syngas. Based on their results, 20%Mn/20%Zr-Al reveals great redox activity, good structural properties, and stability with a methane conversion of about 97.0% at 650 °C and 99.9% at 750 °C. The significantly higher activity of 20Mn/20Zr-Al oxygen carrier could be due to high surface area, better dispersion of manganese oxide, reduction in the particle size of manganese oxide and the superior interactions between Mn and Zr-Al. The reduction in  $\text{H}_2/\text{CO}$  molar ratio with temperature for Zr promoted samples could be related to reverse water gas shift reaction, which increases the concentration of carbon monoxide with the consumption of hydrogen. A maximum of methane and carbon dioxide conversion is obviously obtained by increasing the Mn loading percentage up to 20%. Correspondingly, the catalytic activity is decreased by further increase of active phase loading. Further increase in Mn loading percentage might intensify the agglomeration and pore blockage, which has negative effect on its activity.

### 3.6. Co-based oxygen carries

In general, Co has a few oxidation states such as  $\text{Co}_3\text{O}_4$ , CoO and Co during the redox operation. At a temperature higher than 1173 K,  $\text{Co}_3\text{O}_4$  is unstable and easily convert into CoO. Among the possible metal oxides for chemical looping technology, cobalt shows the highest oxygen transport capability (Hossain & de Lasa, 2008). Therefore, Co-based material might be better choice from an oxygen transport capacity point of view. High melting temperature and fast reactivity are other advantages of this type of material. However, their drawbacks include negative health effects and high cost which limits their

application in large-scale operations (Abuelgasim et al., 2021). The existing literature pertaining to the production of syngas from chemical looping technologies over Co-based material remains scarce.

Dry reforming of methane was studied using  $\text{CeO}_2$ -supported Co catalyst in a fixed bed reactor by (Ayodele et al., 2016). Their results revealed that 20wt%Co/80wt%  $\text{CeO}_2$  has the potential to be used for production of CO-rich hydrogen which is favorable for the production of other value-added chemicals. (D. Li et al., 2018) examined Co catalyst with MgAl support for low-temperature methane reforming and observed that the Co catalyst shows high coke resistance and stable activity due to its lower activity for  $\text{CH}_4$  dissociation/decomposition and its stronger metal-support interaction. (M. Guo et al., 2020) studied the role of Co in chemical looping using iron oxide as an oxygen carrier at a temperature ranging from 600 to 800 °C. As can be seen in **Figure 9**, the methane conversion increased by around 300% for Co-doped iron oxide compared to pure iron oxide oxygen carriers. Furthermore, Co-doping-induced oxygen vacancy significantly reduces energy barriers of  $\text{CH}_4$  reforming on the surface of iron oxide oxygen carriers, leading to reactivity enhancement.

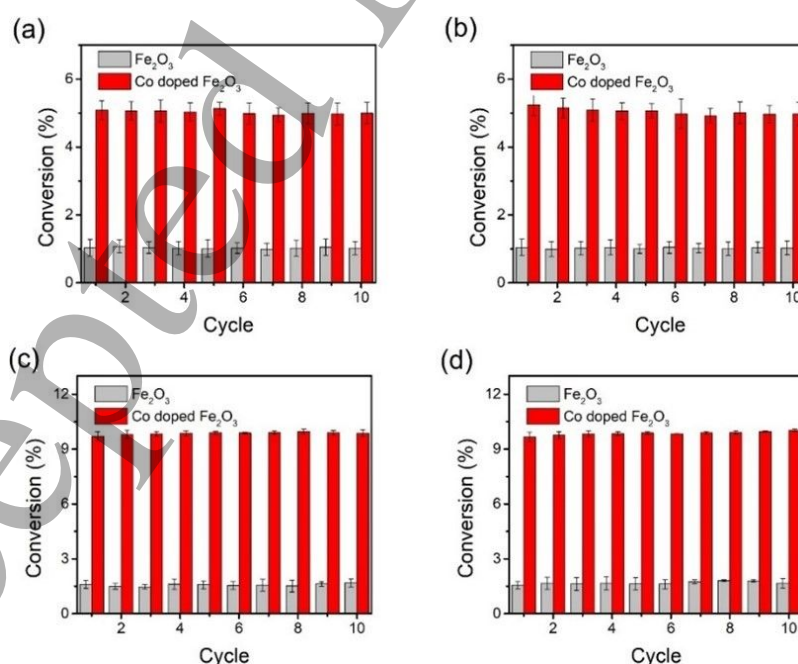


**Figure 9.** The effect of the addition of 2% cobalt to iron-based oxygen carrier in chemical looping reforming at 600 °C for, a) reduction and b) oxidation, at 700 °C for c) reduction and d) oxidation. Reprinted with permission from (M. Guo et al., 2020). 2019, Elsevier.

### 3.7. Mixed oxides as oxygen carries

There is always motivation in finding new alternative catalysts to enhance the chemical looping efficiency. In recent years, many researchers have been exploring the effect of the combination of various metals as a useful technique to improve the characteristics of oxygen carriers in terms of better catalytic activities, improved material mechanical strength, higher product selectivity, and minimizing carbon deposition (Jiao et al., 2017). Mixed metal oxides have been studied extensively for their use in chemical looping technologies. (J. Huang et al., 2019) prepared mixed oxides by impregnating CuO and NiO on  $\alpha$ -Al<sub>2</sub>O<sub>3</sub> supports for chemical looping operation as given in **Figure 10** and observed that Ni-Cu-Al<sub>2</sub>O<sub>3</sub> contains highly active redox-active lattice oxygen when compared to NiO or CuO.

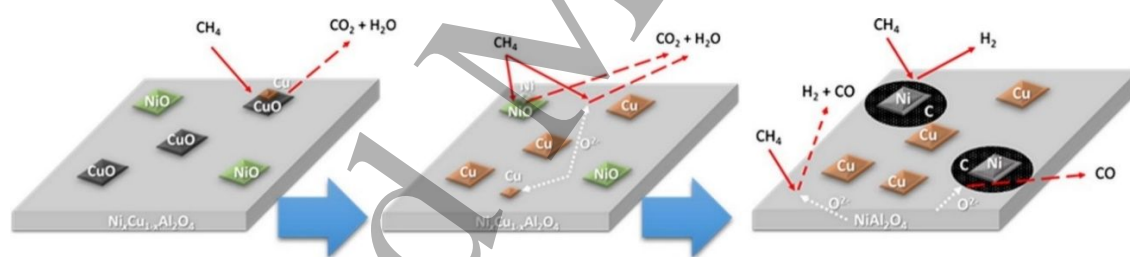


**Figure 10.** A schematic diagram of the reaction sequence. Reprinted with permission from (J. Huang et al., 2019). 2018, Elsevier.

(Khazouz et al., 2013) compared the activity of Cu-modified Ni/Al<sub>2</sub>O<sub>3</sub> with pure Ni/Al<sub>2</sub>O<sub>3</sub> and concluded that the tested Cu-Ni/Al<sub>2</sub>O<sub>3</sub> presents higher H<sub>2</sub> selectivity and lower CO selectivity compared to Ni/Al<sub>2</sub>O<sub>3</sub>. (Rahbar Shamskar et al., 2017) modified 25%Ni/Al<sub>2</sub>O<sub>3</sub> by addition of 1 to 5% Ce in a methane reforming reactor. Ce was chosen due to its great role in the stabilization of the alumina structure at high temperatures and the mobility of surface oxygen. Based on their results, the addition of Ce at a low

amount, less than 2%, can increase the performance of the catalyst due to an improvement in the dispersion of Ni active sites with no sintering of active sites. In general, a combination of  $\text{CeO}_2$  and  $\text{Fe}_2\text{O}_3$  was suggested in the literature as a promising oxygen carrier for the chemical looping reforming of methane. The formation Ce-Fe-O solid solution can improve the thermal stability and oxygen storage capacity of  $\text{CeO}_2$ , which is attributed to the formation of oxygen vacancies. This high cyclic stability in various reactions and high catalytic activity is explained by two reasons: the formation of Ce-Fe-O solid solution and strong interaction between  $\text{Fe}_2\text{O}_3$  and  $\text{CeO}_2$ . It was reported that CuO modified  $\text{Fe}_2\text{O}_3$  exhibits a less coke deposition of material due to partial coverage of CuO with a low propensity for coke formation while maintaining high hydrogen yields over many redox cycles.

(Z. Huang et al., 2016) investigated the crystal structures of Ni-Fe oxygen carriers without inert components. As it can be seen from **Figure 11**, the surface of fresh oxygen carrier particles is constituted of grains with sizes below 5  $\mu\text{m}$  and indicates a good porosity, which is beneficial to the diffusion of gas molecules into the particles inner, increasing their reactivity. No important changes in the surface were detected after 1 cycle while after five cycles it can be observed that the particles surface is apparently worsened, and particle sizes grow to form agglomeration which means the thermal sintering appears on the oxygen carrier surface. The agglomeration is becoming more serious after ten cycles and the porosity disappears, and cracks appear due to the cumulative thermal stress.



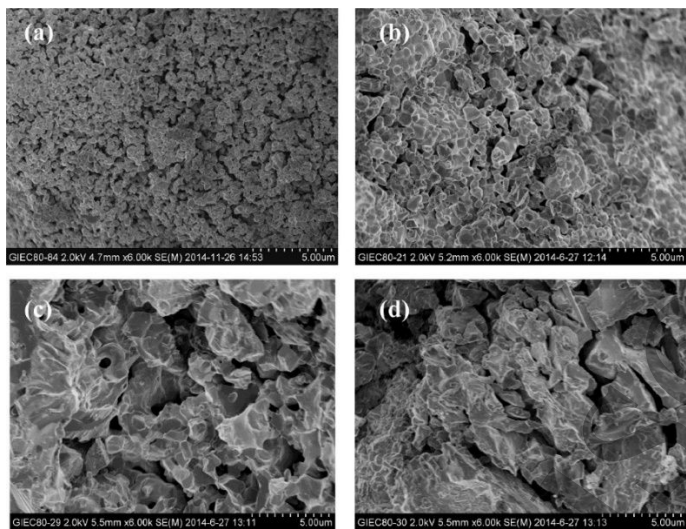


**Figure 11.** SEM images of the fresh and reacted oxygen carrier particles. (a) Fresh, (b) 1st cycle, (c) 5th cycle and (d) 10th cycle. Reprinted with permission from (Z. Huang et al., 2016). 2015, Elsevier.

**3.8. Oxygen carriers with CO<sub>2</sub> sorbent**

The steam reforming reaction releases hydrogen from the fuel, but also releases carbon in the form of CO<sub>2</sub>. Steam methane reforming releases around 10-12 kg CO<sub>2</sub> for each kg of H<sub>2</sub> produced (Ozbilen et al., 2013). Sorption-enhanced steam methane reforming (SE-SMR) unit is one of the intensified paths for the conversion of natural gas directly to high-purity hydrogen. This process combines the reforming reaction system in a single reactor with the addition of a high-temperature solid sorbent. The capture of CO<sub>2</sub> directly as it is produced, overcomes the equilibrium limitations of the WGS and reforming reactions and leads to remarkable improvement of the reactant conversion (Antzaras & Lemonidou, 2022). Furthermore, enhanced hydrogen selectivity is attained in a single step, as a result of shifting the equilibrium of the overall reaction to the product side. Adding CO<sub>2</sub> capture to a steam methane reforming unit increases the cost of H<sub>2</sub> production by 32.5% and reduces net CO<sub>2</sub> emissions by 72-83%. Since the cost of H<sub>2</sub> production is very sensitive to natural gas prices, its variation might greatly affect the costs of both H<sub>2</sub> production and CO<sub>2</sub> capture. It is critical to develop new materials which are capable of



selectively capturing CO<sub>2</sub> under reaction conditions. There are three main categories of CO<sub>2</sub> sorbents including a) low-temperature (less than 200 °C) material such as solid amine, carbon, silica and zeolite-based materials; b) intermediate-temperature (200-450 °C) such as Layered Double Hydroxide and MgO-based materials; and c) high-temperature (450-700 °C) sorbents such as alkaline metal-based and calcium-based materials (Antzaras & Lemonidou, 2022). CaO, MgO and Li<sub>2</sub>ZrO<sub>3</sub> are the most popular CO<sub>2</sub> sorbents in chemical looping reforming units.

Alkaline-based sorbents such as alkaline silicates (Li<sub>4</sub>SiO<sub>4</sub>, CaSiO<sub>3</sub>) or zirconates (Li<sub>2</sub>ZrO<sub>3</sub>, Na<sub>2</sub>ZrO<sub>3</sub>) have several advantages such as the high theoretical sorption capacity, the enhanced stability in multicycle operation and the relatively low temperatures required for regeneration (<750 °C) (Mendoza-Nieto et al., 2018). Li<sub>4</sub>SiO<sub>4</sub> sorbents have high CO<sub>2</sub> absorption capacity at temperatures of 600 to 700 °C under high CO<sub>2</sub> concentration. However, they demonstrate inferior CO<sub>2</sub> capture properties when low CO<sub>2</sub> concentrations (10–20 vol %) are applied, indicating this kind of sorbents might not be an attractive candidate in sorption-enhanced reforming at CO<sub>2</sub> partial pressure below 0.15 bar due to the constraint on the external CO<sub>2</sub> diffusion to the surface of the particles. The incorporation of ions (Na, K, Ce, Mg, Ca) in the silicate structure can improve their performance at low CO<sub>2</sub> concentrations. In terms of sorption capacity, Li<sub>4</sub>SiO<sub>4</sub> (8 mol CO<sub>2</sub>/kg sorbent) shows twice as much sorption capacity compared to Li<sub>2</sub>ZrO<sub>3</sub> (4.5 mol CO<sub>2</sub>/kg sorbent) and Na<sub>2</sub>ZrO<sub>3</sub> (3.5 mol CO<sub>2</sub>/kg sorbent).

Thanks to the advantages of CaO such as cheap price, fast carbonation kinetics, their wide availability and high theoretical sorption capacity (17 mol CO<sub>2</sub>/kg sorbent), CO<sub>2</sub> sorbents attracted much attention for high-temperature applications (Abanades & Alvarez, 2003). (Dou et al., 2018) used a fixed-bed reactor to study the effect of CaO sorbent/NiO catalyst on product composition. They showed that the addition of the optimized amount of CaO-based sorbent in ethanol reforming has a positive effect on process performances and heat supply.

decay in activity of CaO-based sorbents due to sintering during the calcination process was one of the limitations of this technology. The addition of steam during the carbonation step has also been reported to enhance the performance of CaO-based sorbents. One possible mechanism is based on the catalytic influence of steam, by which the production of surface  $-OH$  groups and bicarbonates may play an important role as intermediates and lead to enhanced carbonation of CaO.

Dolomite can be considered a promising  $CO_2$  sorbent material, as it presents fast reaction rates, low cost and adequate stability compared to limestone. Magnesium oxides (MgO) are another attractive  $CO_2$  sorbent due to their moderate  $CO_2$  sorption capacity, wide availability, low price, highly reactive towards  $CO_2$ , and good  $CO_2$  sorption capacity at 300-450 °C and high pressure (Dou et al. 2016). (Dang et al., 2020) prepared porous microsphere Ni-CaO-MgO bifunctional material by hydrothermal method and tested it in a glycerol reforming system at 550 °C and S/C of 4. They showed that CaO-MgO had good  $CO_2$  sorption performance. After 10 cycles of sorption/desorption, the  $H_2$  purity was more than 96%, showing excellent potential for promoting hydrogen production.

(Martini, Druiff, et al., 2021) successfully demonstrated a sorption-enhanced steam reforming of methane at the TRL5 scale. Ca-based solid, Ni-catalyst and Cu-based material were used as  $CO_2$  sorbent, reforming catalyst and oxygen carrier, respectively. It was found an increase in pressure negatively affects the sorption-enhanced reforming step by decreasing the purity of  $H_2$  in the outlet stream. Furthermore, the average outlet  $H_2$  fraction was not a strong function of the steam-to-carbon ratio. Increasing hydrogen fraction in the feed during the regeneration step from 20 vol% to 60 vol% resulted in an increase in the amount of regenerated sorbent from 53 wt% to 70 wt%. It was reported that after even 285 cycles, the solids were still chemically performing well, and the results were still reproducible. The same authors in another work (Martini, Jain, et al., 2021) showed that a temperature range of 600 to 650 °C was found to be the most appropriate for optimal performance of the sorption-enhanced reforming

step. As temperature rises, carbonation and water gas shift reactions are relatively slow which leads to a significant CO exit fraction and a longer breakthrough period until the CaO sorbent is completely saturated. Furthermore, their experimental results revealed that a bed containing 27.5 wt% catalysts and 72.5 wt% sorbent is required for optimum reactor performance.

The major conclusions are drawn as follows:

- It is critical to select a suitable oxygen carrier based on its thermal stability to avoid material sintering.
- Toxicity and coke formation on the surface of Ni lead to blockage of nickel active sites and deactivation.
- In CLR processes, material deactivation caused by carbon deposition is one of the main issues.
- The oxygen carriers prepared by dry impregnation exhibit a lower tendency to increase the carbon deposition than the oxygen carriers prepared by a deposition-precipitation.
- SiO<sub>2</sub> and Al<sub>2</sub>O<sub>3</sub> indicated excellent stability at high temperature.
- Among Ni, Co and Cu active metals, the highest glycerol conversion and the hydrogen selectivity were obtained by Ni/SiO<sub>2</sub> while Ni/Al<sub>2</sub>O<sub>3</sub> catalyst exhibited the highest H<sub>2</sub>/CO and the lowest CO/CO<sub>2</sub> ratio.
- By adding inert supports and using different preparation method, the performance of Cu-based material can be improved at high temperatures.
- The combination of various metal oxides is a useful technique to improve the characteristics of oxygen carriers in terms of catalytic activities, material mechanical strength, product selectivity, and minimizing carbon deposition.

- Among the possible metal oxides in CLR technology, cobalt shows the highest oxygen transport capability.
- $\text{Li}_2\text{ZrO}_3$  sorbents are attractive candidates at high  $\text{CO}_2$  concentrations while  $\text{CaO}$  offer good performance for high-temperature application.

#### 4. Thermodynamic analysis

The reduction of metal oxides at different temperatures is important to screen suitable oxygen carrier candidates and operational conditions in chemical looping reforming. The selection of metal oxides can be made based on a modified Ellingham diagram, where the standard Gibbs free energy change variations with the temperature as shown in Fig. 12 (Fan et al., 2015b). A minimization of total Gibbs free energy is a suitable approach to determine the equilibrium compositions of any reacting system.

It can be observed that Mn is more easily oxidized compared to Fe and it is thermodynamically favorable for Mn to be oxidized by  $\text{O}_2$  to  $\text{MnO}$  in temperatures up to 1600 °C (Vos et al., 2020a). The complete sequence in order of easiness of oxidation for all transition metals suitable for chemical looping can be ordered as follow  $\text{Mn} > \text{Fe} > \text{Co} > \text{Ni} > \text{Cu}$ . Metals that are more difficult to be oxidized compared to Cu are not suitable for chemical looping since they are not regenerable by air. The metals that are easier to be oxidized compared to Mn become too difficult to reduce with fuel.

Furthermore, the trend from Mn to Cu shows the suitability of the metal/metal oxide pairs for certain chemical looping technologies. While Fe/FeO is more viable for syngas generation by chemical looping reforming, the transformation between CuO and Cu is utilized much more frequently for chemical looping combustion. As the Gibbs free energy for the oxidation of this Cu/CuO pair is almost zero, it is even eligible for chemical looping with oxygen uncoupling (Vos et al., 2020a).

(X. Wang et al., 2009) performed the thermodynamics study of glycerol reforming for syngas and  $H_2$  generation. Through the Gibbs free energy minimization method, the optimum conditions were obtained at  $CO_2$ /glycerol ratios of 0 to 1 with reaction temperatures higher than 702 °C. Reaction at high pressure and  $CO_2$  loading also gives a negative impact on the  $H_2$  and syngas yields. (Shah et al., 2021) analyzed reforming of methane using  $Ca_2Fe_2O_5$  as an oxygen carrier and showed that the change in Gibbs free energy for partial oxidation is much more negative in comparison to that of complete oxidation reaction, indicating partial oxidation of  $CH_4$  using  $Ca_2Fe_2O_5$  to form syngas is thermodynamically favoured. At temperatures higher than 683 °C,  $CH_4$  reacts with the oxygen carrier to form a limited amount of  $CO_2$ . It was found that the change in Gibbs free energy for partial oxidation of  $CH_4$  using  $Fe_2O_3$  was less negative compared to  $Ca_2Fe_2O_5$ , implying the thermodynamic superiority of the CaO-modified  $Fe_2O_3$ .

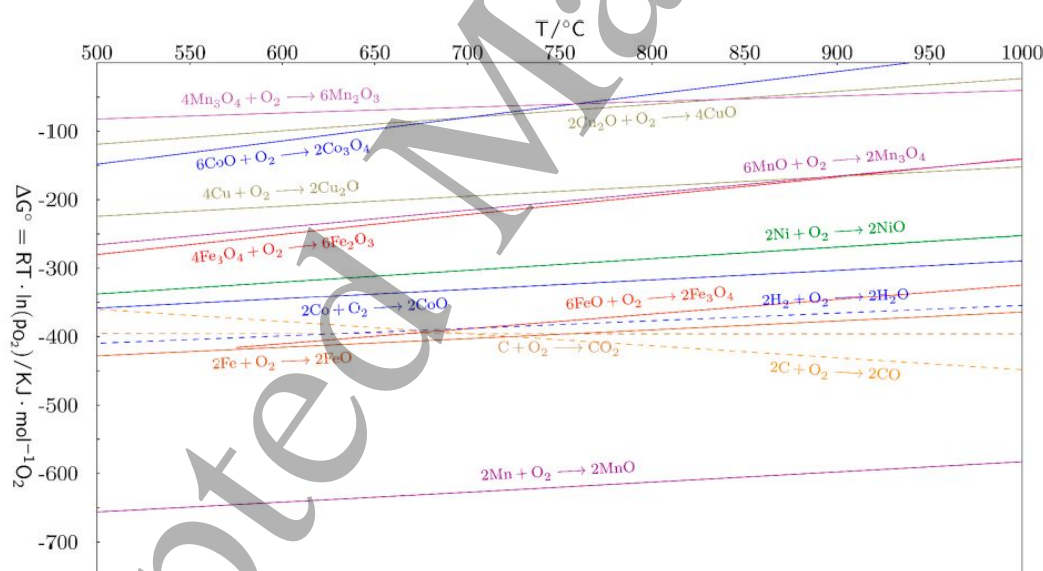


**Fig. 12.** Ellingham diagram of different metal oxides. Reprinted from (Vos et al., 2020a)

## 5. Membrane-assisted chemical looping reforming

The concept of a membrane-assisted chemical looping hybrid process to produce  $H_2$  with high quality has been for the first time performed by the group of Gallucci (Gallucci et al., 2008a)(Gallucci et al.,

2008b) and van Sint Annaland (Patil et al., 2007). In this approach, the fuel reactor of the chemical looping reforming process is coupled to H<sub>2</sub>-permeated membranes. The combination of these two technologies has the potential of merging in an efficient way with direct CO<sub>2</sub> capture and pure H<sub>2</sub> production. (Spallina, Pandolfo, et al., 2016) proposed a membrane-assisted chemical looping reforming plant for pure H<sub>2</sub> production. In this system, methane is converted in the fuel reactor by reaction with steam and produces syngas. The oxygen carriers that act as a catalyst for both SMR and WGS reactions can be transported to the air reactor. The produced hydrogen is directly recovered from the fuel reactor via hydrogen-selective membranes immersed in this fluidized bed fuel reactor. The H<sub>2</sub> production efficiency of the membrane-assisted chemical looping reforming was obtained to be more than 90%, which is 30% higher than conventional fired tubular reforming with CO<sub>2</sub> absorption technology based on MDEA solution. (Medrano et al., 2014) conducted a comparison between membrane-assisted chemical looping reforming (MA-CLR) with conventional steam methane reforming coupled with chemical looping combustion (SMR-CLC), CLR and fluidized bed membrane reactor (FBMR). Their thermodynamic analysis has been carried out under different conditions such as reforming temperature, operating pressure and S/C ratio. As depicted in **Figure 12**, compared to CLR, the main advantage is the possibility to obtain a high fuel conversion and thus a high performance at low temperatures due to the presence of the membranes. Furthermore, their investigation showed that at a lower temperature (600-700 °C) the FBMR and the MA-CLR exhibit a reforming efficiency in the range of 75-90% which is significantly higher than CLR and SMR. It FBMR and MA-CLR presented almost the same performance by increasing temperature. In another work, (Medrano et al., 2018) successfully demonstrated membrane-assisted methane reforming in which pure H<sub>2</sub> was separated from the fuel reactor through palladium-based membranes as shown in **Figure 12**. Methane conversion above 90% was determined with the use of Ni-based catalyst as an oxygen carrier at 600 °C.

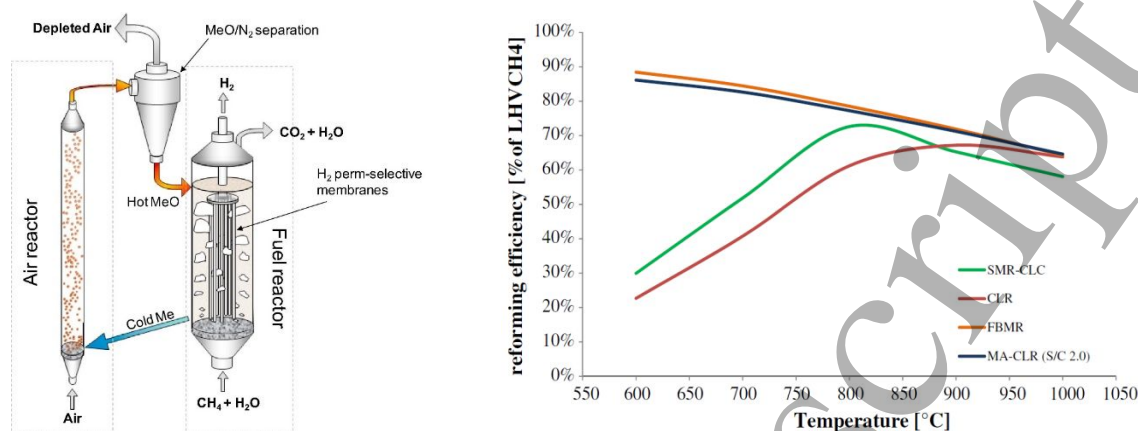


**Figure 13 .** Schematic representation of MA-CLR system (left) and profile of reforming efficiency of the systems studied as a function of the reactor temperature (right). Reprinted with permission from (Medrano et al., 2014) (Medrano et al., 2018). 2013 Elsevier.

To achieve an economically viable chemical looping process, the cost of the oxygen carrier (and thus, at large scale production, especially the cost of the raw materials) is of vital importance (Vos et al., 2020b). (L. Zhu et al., 2018) assessed the techno-economic performance of a chemical looping plant employing different oxygen carriers. The corresponding levelized cost of electricity ranged from 75 to 89 \$/MWh, in which nickel has the lowest levelized cost of electricity followed by copper. They showed that a rise in pressure from 6 bar to 18 bar initially decreased the cost of electricity from 105.3 to 74.5 \$/MWh). (Nazir et al., 2018) evaluated a CLR plant integrated with a combined cycle power plant. The plant was operated at 18 bar and utilized a Ni-based material as oxygen carrier. The syngas produced in the CLR was subjected to water gas shift reaction before absorbing the CO<sub>2</sub> in a amine solution. A comprehensive sensitivity study indicated that the net electrical efficiencies ranged between 40 and 43.4% while the levelized cost of electricity varied between 132.7 and 145.9 \$/MWh. (Spallina, Pandolfo, et al., 2016) conducted a techno-economic assessment of a membrane-based CLR plant integrated with CO<sub>2</sub> capture. The operating pressure were in a range of 32 to 50 bar. Oxygen carrier reduction and methane reforming

to syngas occur in the fuel reactor, while the produced hydrogen permeates through the membranes for separation. The plant exhibited low energy cost for CO<sub>2</sub> separation and compression which makes the overall reforming efficiency up to 20% higher than the conventional fired tubular reforming with CO<sub>2</sub> separation. Furthermore, the cost of hydrogen production decreased from 0.28 €/Nm<sup>3</sup><sub>H<sub>2</sub></sub> to 0.19 €/Nm<sup>3</sup><sub>H<sub>2</sub></sub>. (Spallina et al., 2019) performed a full-scale techno-economic analysis of a chemical looping based process using dynamically operated packed bed reactors for the large-scale production of hydrogen (up to 30,000 Nm<sup>3</sup>/h). Compared to a conventional H<sub>2</sub> production plant, the reforming efficiency was found to be 3% higher, while the required primary energy consumption to separate CO<sub>2</sub> was reported to be 0.47 MJLHV/kg<sub>CO<sub>2</sub></sub> which is significantly lower than that of an amine-based plant (> 1.35 MJLHV/kg<sub>CO<sub>2</sub></sub>). Moreover, it was found that the cost of hydrogen production with the proposed process is 2.19 \$/kg with a CO<sub>2</sub> avoidance cost of 58.7 \$/ton<sub>CO<sub>2</sub></sub> (compared to > 70.6 \$/ton<sub>CO<sub>2</sub></sub> for solvent-based plant).

## 6. Conclusion

CLR is considered an emerging technology with the main advantage being the indirect contact of the fuel with the oxidant by means of an oxygen transfer material. In this work, the state-of-the-art oxygen carriers, and CO<sub>2</sub> sorbents in chemical looping reforming of methane, ethanol and glycerol were summarised. The influence of key process variables controlling the CLR such as reactor temperature, pressure, water/fuel ratio and CO<sub>2</sub>/fuel ratio on fuel conversion and syngas quality was assessed. The key messages of this work can be summarized as follows:

- The methane conversion was found to be sensitive to the operating temperature below 800 °C.
- Co-feeding CO<sub>2</sub> into the fuel reactor was used to adjust the H<sub>2</sub>/CO-ratio of the syngas, but a risk of coke formation in the bottom of the fuel reactor still exists.



- The high temperatures, high steam-to-glycerol ratios and low oxygen-to-glycerol ratios are feasible for glycerol reforming. In glycerol reforming, the temperature optimal is always somewhere around 650–900 °C, while pressure is always kept low.
- The design and configuration of a reactor have an important role in product yield and process efficiency.
- From good heat and mass transfer behavior point of view, the fluidized bed reactor presents better performance compared to a moving bed or fixed bed reactor, while moving bed reactors offer better control over fuel utilization and conversions of the looping carrier.
- The development of the oxygen carrier with high selectivity, great stability, fast reactivity and resistance against carbon deposition are the key aspects of the successful operation of CLR.
- The preparation method of the catalyst plays a key role in the performance of the catalyst. The suitable and proper preparation method could give higher Ni dispersion on support, strong metal-support interaction, high catalytic activity, stability, and high resistance to carbon formation.
- Ce-based OCs are thermodynamically favored for preferentially oxidizing methane to syngas at low temperatures, but their redox stability and oxygen storage capacity need to be improved.
- Cu-based oxygen carriers are suitable for temperatures less than 1000 °C. They showed high oxygen transport capacity and high activity for complete oxidation of methane and strong resistance to carbon deposition.
- Ni is probably the best oxygen carrier for the steam reforming of glycerol. It offers high reactivity and stability during multi-redox cycles. However, carbon formation is easily generated on Ni-based oxygen carriers when carbon-containing fuels are used. Doping an impurity and adding a proportion of steam into the fuels can inhibit carbon formation.

- Type of catalyst support, mixed materials, using suitable catalyst preparation methods, the addition of promoters, modify particle size can be used to improve oxygen carrier characteristics.
- CaO-based solids and alkaline-based materials ( $\text{Li}_2\text{ZrO}_3$ ,  $\text{Li}_4\text{SiO}_4$ ,  $\text{Na}_2\text{ZrO}_3$ ) are the most attractive  $\text{CO}_2$  sorbent materials due to their application at relatively high temperatures. .
- The sorption-enhanced chemical looping reforming concept has the potential to be considered an attractive technology for the production of hydrogen with  $\text{H}_2$  purity of more than 98% and zero  $\text{CO}_2$  emission.
- There are still challenges to be overcome in industrial applications, such as stabilizing the continuous long operation of the chemical looping process, controlling the proper heat balance between the oxidizer and reducer, and maintaining the recyclability properties of the oxygen carriers.

## Acknowledgment



This project has received funding from the European Union's Horizon 2020 research and innovation program under grant agreement No 884197 (GLAMOUR).

## Data availability statement

The data that support the findings of this study are available upon reasonable request from the authors.

## Conflict of interest

The authors have declared that no competing interests exist.

## ORCID iDs

Rouzbeh Ramezani <https://orcid.org/0000-0002-9234-4470>

Luca Di Felice <https://orcid.org/0000-0002-4378-6408>

Fausto Gallucci <https://orcid.org/0000-0001-6379-773X>

## References

- Abad, A., Adánez, J., García-Labiano, F., de Diego, L. F., Gayán, P., & Celaya, J. (2007). Mapping of the range of operational conditions for Cu-, Fe-, and Ni-based oxygen carriers in chemical-looping combustion. *Chemical Engineering Science*, 62(1–2), 533–549. <https://doi.org/10.1016/J.CES.2006.09.019>
- Abanades, J. C., & Alvarez, D. (2003). *Conversion Limits in the Reaction of CO 2 with Lime*. <https://doi.org/10.1021/ef020152a>
- Abdalazeez, A., Wang, W., & Abuelgasim, S. (2021). Syngas production from chemical looping reforming of ethanol over iron-based oxygen carriers: Theoretical analysis and experimental investigation. *Chinese Journal of Chemical Engineering*, 38, 123–131. <https://doi.org/10.1016/j.cjche.2021.02.012>
- Abuelgasim, S., Wang, W., & Abdalazeez, A. (2021). A brief review for chemical looping combustion as a promising CO2 capture technology: Fundamentals and progress. *Science of the Total Environment*, 764. <https://doi.org/10.1016/J.SCITOTENV.2020.142892>
- Adanez, J., Abad, A., Garcia-Labiano, F., Gayan, P., & de Diego, L. F. (2012). Progress in chemical-looping combustion and reforming technologies. *Progress in Energy and Combustion Science*, 38(2), 215–282. <https://doi.org/10.1016/J.PECS.2011.09.001>
- Adánez, J., Abad, A., Mendiara, T., Gayán, P., de Diego, L. F., & García-Labiano, F. (2018). Chemical looping combustion of solid fuels. *Progress in Energy and Combustion Science*, 65, 6–66. <https://doi.org/10.1016/J.PECS.2017.07.005>
- Adánez-Rubio, I., Bararpour, S. T., Abad, A., Gayán, P., Williams, G., Scullard, A., Mahinpey, N., & Adánez, J. (2020). Performance Evaluation of a Cu-Based Oxygen Carrier Impregnated onto ZrO2 for Chemical-Looping Combustion (CLC). *Industrial and Engineering Chemistry Research*, 59(15), 7255–7266. <https://doi.org/10.1021/acs.iecr.9b05835>
- Adánez-Rubio, I., Ruiz, J. A. C., García-Labiano, F., de Diego, L. F., & Adánez, J. (2021). Use of bio-glycerol for the production of synthesis gas by chemical looping reforming. *Fuel*, 288. <https://doi.org/10.1016/j.fuel.2020.119578>
- Adhikari, S., Fernando, S., & Haryanto, A. (2007). Production of hydrogen by steam reforming of glycerin over alumina-supported metal catalysts. *Catalysis Today*, 129(3–4), 355–364. <https://doi.org/10.1016/J.CATTOD.2006.09.038>
- Alam, S., Kumar, J. P., Rani, K. Y., & Sumana, C. (2020). Comparative assessment of performances of different oxygen carriers in a chemical looping combustion coupled intensified reforming process through simulation study. *Journal of Cleaner Production*, 262. <https://doi.org/10.1016/J.JCLEPRO.2020.121146>
- Alexandros Argyris, P., de Leeuwe, C., Abbas, S. Z., Amieiro, A., Poulton, S., Wails, D., & Spallina, V. (2022). Chemical looping reforming for syngas generation at real process conditions in packed bed reactors: An

experimental demonstration. *Chemical Engineering Journal*, 435, 134883.  
<https://doi.org/10.1016/J.CEJ.2022.134883>

Alirezaei, I., Hafizi, A., & Rahimpour, M. R. (2018a). Syngas production in chemical looping reforming process over ZrO<sub>2</sub> promoted Mn-based catalyst. *Journal of CO<sub>2</sub> Utilization*, 23, 105–116.  
<https://doi.org/10.1016/J.JCOU.2017.09.010>

Alirezaei, I., Hafizi, A., & Rahimpour, M. R. (2018b). Syngas production in chemical looping reforming process over ZrO<sub>2</sub> promoted Mn-based catalyst. *Journal of CO<sub>2</sub> Utilization*, 23, 105–116.  
<https://doi.org/10.1016/j.jcou.2017.09.010>

Alirezaei, I., Hafizi, A., Rahimpour, M. R., & Raeissi, S. (2016). Application of zirconium modified Cu-based oxygen carrier in chemical looping reforming. *Journal of CO<sub>2</sub> Utilization*, 14, 112–121.  
<https://doi.org/10.1016/j.jcou.2016.04.007>

Alizadeh Sahraei, O., Desgagnés, A., Larachi, F., & Iliuta, M. C. (2021). A comparative study on the performance of M (Rh, Ru, Ni)-promoted metallurgical waste driven catalysts for H<sub>2</sub> production by glycerol steam reforming. *International Journal of Hydrogen Energy*, 46(63), 32017–32035.  
<https://doi.org/10.1016/J.IJHYDENE.2021.06.192>

Antzara, A., Heracleous, E., Silvester, L., Bukur, D. B., & Lemonidou, A. A. (2016). Activity study of NiO-based oxygen carriers in chemical looping steam methane reforming. *Catalysis Today*, 272, 32–41.  
<https://doi.org/10.1016/j.cattod.2015.10.027>

Antzaras, A. N., & Lemonidou, A. A. (2022). Recent advances on materials and processes for intensified production of blue hydrogen. *Renewable and Sustainable Energy Reviews*, 155.  
<https://doi.org/10.1016/J.RSER.2021.111917>

Argyris, P. A., Wright, A., Taheri Qazvini, O., & Spallina, V. (2022). Dynamic behaviour of integrated chemical looping process with pressure swing adsorption in small scale on-site H<sub>2</sub> and pure CO<sub>2</sub> production. *Chemical Engineering Journal*, 428. <https://doi.org/10.1016/j.cej.2021.132606>

Atilhan, S., Park, S., El-Halwagi, M. M., Atilhan, M., Moore, M., & Nielsen, R. B. (2021). Green hydrogen as an alternative fuel for the shipping industry. *Current Opinion in Chemical Engineering*, 31.  
<https://doi.org/10.1016/J.COCH.2020.100668>

Ayodele, B. v., Khan, M. R., & Cheng, C. K. (2016). Catalytic performance of ceria-supported cobalt catalyst for CO-rich hydrogen production from dry reforming of methane. *International Journal of Hydrogen Energy*, 41(1), 198–207. <https://doi.org/10.1016/J.IJHYDENE.2015.10.049>

Bao, J., Li, Z., & Cai, N. (2014). Interaction between iron-based oxygen carrier and four coal ashes during chemical looping combustion. *Applied Energy*, 115, 549–558.  
<https://doi.org/10.1016/J.APENERGY.2013.10.051>

- Barreto, L., Makihiro, A., & Riahi, K. (2003). The hydrogen economy in the 21st century: a sustainable development scenario. *International Journal of Hydrogen Energy*, 28(3), 267–284. [https://doi.org/10.1016/S0360-3199\(02\)00074-5](https://doi.org/10.1016/S0360-3199(02)00074-5)
- Baykara, S. Z. (2018). Hydrogen: A brief overview on its sources, production and environmental impact. *International Journal of Hydrogen Energy*, 43(23), 10605–10614. <https://doi.org/10.1016/J.IJHYDENE.2018.02.022>
- Byrd, A. J., Pant, K. K., & Gupta, R. B. (2008). Hydrogen production from glycerol by reforming in supercritical water over Ru/Al<sub>2</sub>O<sub>3</sub> catalyst. *Fuel*, 87(13–14), 2956–2960. <https://doi.org/10.1016/J.FUEL.2008.04.024>
- Charisiou, N. D., Italiano, C., Pino, L., Sebastian, V., Vita, A., & Goula, M. A. (2020). Hydrogen production via steam reforming of glycerol over Rh/ $\gamma$ -Al<sub>2</sub>O<sub>3</sub> catalysts modified with CeO<sub>2</sub>, MgO or La<sub>2</sub>O<sub>3</sub>. *Renewable Energy*, 162, 908–925. <https://doi.org/10.1016/J.RENENE.2020.08.037>
- Chaubey, R., Sahu, S., James, O. O., & Maity, S. (2013). A review on development of industrial processes and emerging techniques for production of hydrogen from renewable and sustainable sources. *Renewable and Sustainable Energy Reviews*, 23, 443–462. <https://doi.org/10.1016/J.RSER.2013.02.019>
- Chein, R. Y., & Fung, W. Y. (2019). Syngas production via dry reforming of methane over CeO<sub>2</sub> modified Ni/Al<sub>2</sub>O<sub>3</sub> catalysts. *International Journal of Hydrogen Energy*, 44(28), 14303–14315. <https://doi.org/10.1016/J.IJHYDENE.2019.01.113>
- Chen, H., Ding, Y., Cong, N. T., Dou, B., Dupont, V., Ghadiri, M., & Williams, P. T. (2011). A comparative study on hydrogen production from steam-glycerol reforming: thermodynamics and experimental. *Renewable Energy*, 36(2), 779–788. <https://doi.org/10.1016/J.RENENE.2010.07.026>
- Chen, J., Zhao, K., Zhao, Z., He, F., Huang, Z., & Wei, G. (2019). Identifying the roles of MFe<sub>2</sub>O<sub>4</sub> (M=Cu, Ba, Ni, and Co) in the chemical looping reforming of char, pyrolysis gas and tar resulting from biomass pyrolysis. *International Journal of Hydrogen Energy*, 44(10), 4674–4687. <https://doi.org/10.1016/j.ijhydene.2018.12.216>
- Cheng, Z., Qin, L., Fan, J. A., & Fan, L. S. (2018). New Insight into the Development of Oxygen Carrier Materials for Chemical Looping Systems. *Engineering*, 4(3), 343–351. <https://doi.org/10.1016/J.ENG.2018.05.002>
- Cheng, Z., Zhang, L., Jin, N., Zhu, Y., Chen, L., Yang, Q., Yan, M., Ma, X., & Wang, X. (2021). Effect of calcination temperature on the performance of hexaaluminate supported CeO<sub>2</sub> for chemical looping dry reforming. *Fuel Processing Technology*, 218, 106873. <https://doi.org/10.1016/J.FUPROC.2021.106873>
- Chiron, F. X., & Patience, G. S. (2012). Kinetics of mixed copper–iron based oxygen carriers for hydrogen production by chemical looping water splitting. *International Journal of Hydrogen Energy*, 37(14), 10526–10538. <https://doi.org/10.1016/J.IJHYDENE.2012.04.052>

- Dai, X. P., Li, J., Fan, J. T., Wei, W. S., & Xu, J. (2012). Synthesis gas generation by chemical-looping reforming in a circulating fluidized bed reactor using Perovskite LaFeO<sub>3</sub>-based oxygen carriers. *Industrial and Engineering Chemistry Research*, 51(34), 11072–11082.  
[https://doi.org/10.1021/IE300033E/SUPPL\\_FILE/IE300033E\\_SI\\_001.PDF](https://doi.org/10.1021/IE300033E/SUPPL_FILE/IE300033E_SI_001.PDF)
- Dang, C., Liu, L., Yang, G., Cai, W., Long, J., & Yu, H. (2020). Mg-promoted Ni-CaO microsphere as bi-functional catalyst for hydrogen production from sorption-enhanced steam reforming of glycerol. *Chemical Engineering Journal*, 383, 123204. <https://doi.org/10.1016/J.CEJ.2019.123204>
- de Diego, L. F., Ortiz, M., García-Labiano, F., Adánez, J., Abad, A., & Gayán, P. (2009). Hydrogen production by chemical-looping reforming in a circulating fluidized bed reactor using Ni-based oxygen carriers. *Journal of Power Sources*, 192(1), 27–34. <https://doi.org/10.1016/J.JPOWSOUR.2008.11.038>
- Delparish, A., & Avci, A. K. (2016). Intensified catalytic reactors for Fischer-Tropsch synthesis and for reforming of renewable fuels to hydrogen and synthesis gas. *Fuel Processing Technology*, 151, 72–100.  
<https://doi.org/10.1016/J.FUPROC.2016.05.021>
- Delparish, A., Koc, S., Caglayan, B. S., & Avci, A. K. (2019). Oxidative steam reforming of glycerol to synthesis gas in a microchannel reactor. *Catalysis Today*, 323, 200–208. <https://doi.org/10.1016/J.CATTOD.2018.03.047>
- Ding, H., Luo, C., Li, X., Cao, D., Shen, Q., & Zhang, L. (2019). Development of BaSrCo-based perovskite for chemical-looping steam methane reforming: A study on synergistic effects of A-site elements and CeO<sub>2</sub> support. *Fuel*, 253, 311–319. <https://doi.org/10.1016/J.FUEL.2019.04.150>
- Dou, B., Dupont, V., Rickett, G., Blakeman, N., Williams, P. T., Chen, H., Ding, Y., & Ghadiri, M. (2009). Hydrogen production by sorption-enhanced steam reforming of glycerol. *Bioresource Technology*, 100(14), 3540–3547. <https://doi.org/10.1016/J.BIORTECH.2009.02.036>
- Dou, B., Song, Y., Wang, C., Chen, H., Yang, M., & Xu, Y. (2014). Hydrogen production by enhanced-sorption chemical looping steam reforming of glycerol in moving-bed reactors. *Applied Energy*, 130, 342–349.  
<https://doi.org/10.1016/J.APENERGY.2014.05.061>
- Dou, B., Zhang, H., Cui, G., Wang, Z., Jiang, B., Wang, K., Chen, H., & Xu, Y. (2017). Hydrogen production and reduction of Ni-based oxygen carriers during chemical looping steam reforming of ethanol in a fixed-bed reactor. *International Journal of Hydrogen Energy*, 42(42), 26217–26230.  
<https://doi.org/10.1016/J.IJHYDENE.2017.08.208>
- Dou, B., Zhang, H., Cui, G., Wang, Z., Jiang, B., Wang, K., Chen, H., & Xu, Y. (2018). Hydrogen production by sorption-enhanced chemical looping steam reforming of ethanol in an alternating fixed-bed reactor: Sorbent to catalyst ratio dependencies. *Energy Conversion and Management*, 155, 243–252.  
<https://doi.org/10.1016/J.ENCONMAN.2017.10.075>

- Elias, K. F. M., Lucrédio, A. F., & Assaf, E. M. (2013). Effect of CaO addition on acid properties of Ni–Ca/Al<sub>2</sub>O<sub>3</sub> catalysts applied to ethanol steam reforming. *International Journal of Hydrogen Energy*, 38(11), 4407–4417. <https://doi.org/10.1016/J.IJHYDENE.2013.01.162>
- Fan, L. S., Zeng, L., & Luo, S. (2015a). Chemical-looping technology platform. *AIChE Journal*, 61(1), 2–22. <https://doi.org/10.1002/AIC.14695>
- Fan, L. S., Zeng, L., & Luo, S. (2015b). Chemical-looping technology platform. *AIChE Journal*, 61(1), 2–22. <https://doi.org/10.1002/AIC.14695>
- Fan, L. S., Zeng, L., Wang, W., & Luo, S. (2012). Chemical looping processes for CO<sub>2</sub> capture and carbonaceous fuel conversion – prospect and opportunity. *Energy & Environmental Science*, 5(6), 7254–7280. <https://doi.org/10.1039/C2EE03198A>
- Forero, C. R., Gayán, P., García-Labiano, F., de Diego, L. F., Abad, A., & Adánez, J. (2010). Effect of gas composition in Chemical-Looping Combustion with copper-based oxygen carriers: Fate of sulphur. *International Journal of Greenhouse Gas Control*, 4(5), 762–770. <https://doi.org/10.1016/J.IJGGC.2010.04.002>
- Forero, C. R., Gayán, P., García-Labiano, F., de Diego, L. F., Abad, A., & Adánez, J. (2011). High temperature behaviour of a CuO/γAl<sub>2</sub>O<sub>3</sub> oxygen carrier for chemical-looping combustion. *International Journal of Greenhouse Gas Control*, 5(4), 659–667. <https://doi.org/10.1016/J.IJGGC.2011.03.005>
- Forutan, H. R., Karimi, E., Hafizi, A., Rahimpour, M. R., & Keshavarz, P. (2015). Expert representation chemical looping reforming: A comparative study of Fe, Mn, Co and Cu as oxygen carriers supported on Al<sub>2</sub>O<sub>3</sub>. *Journal of Industrial and Engineering Chemistry*, 21, 900–911. <https://doi.org/10.1016/J.JIEC.2014.04.031>
- Gallucci, F., van Sint Annaland, M., & Kuipers, J. A. M. (2008a). Autothermal reforming of methane with integrated CO<sub>2</sub> capture in a novel fluidized bed membrane reactor. Part 1: Experimental demonstration. *Topics in Catalysis*, 51(1–4), 133–145. <https://doi.org/10.1007/S11244-008-9126-8/TABLES/7>
- Gallucci, F., van Sint Annaland, M., & Kuipers, J. A. M. (2008b). Autothermal reforming of methane with integrated CO<sub>2</sub> capture in a novel fluidized bed membrane reactor. Part 2 comparison of reactor configurations. *Topics in Catalysis*, 51(1–4), 146–157. <https://doi.org/10.1007/S11244-008-9127-7/FIGURES/7>
- García-Díez, E., García-Labiano, F., de Diego, L. F., Abad, A., Gayán, P., & Adánez, J. (2017). Autothermal chemical looping reforming process of different fossil liquid fuels. *International Journal of Hydrogen Energy*, 42(19), 13633–13640. <https://doi.org/10.1016/J.IJHYDENE.2016.12.109>
- García-García, F. R., & Metcalfe, I. S. (2021). Chemical looping dry reforming of methane using mixed oxides of iron and cerium: Operation window. *Catalysis Communications*, 160, 106356. <https://doi.org/10.1016/J.CATCOM.2021.106356>

- García-Labiano, F., de Diego, L. F., García-Díez, E., Serrano, A., Abad, A., Gayán, P., & Adanez, J. (2014). Combustion and Reforming of Ethanol in a Chemical Looping Continuous Unit. *Energy Procedia*, 63, 53–62. <https://doi.org/10.1016/J.EGYPRO.2014.11.006>
- García-Labiano, F., García-Díez, E., de Diego, L. F., Serrano, A., Abad, A., Gayán, P., Adánez, J., & Ruíz, J. A. C. (2015a). Syngas/H<sub>2</sub> production from bioethanol in a continuous chemical-looping reforming prototype. *Fuel Processing Technology*, 137, 24–30. <https://doi.org/10.1016/J.FUPROC.2015.03.022>
- García-Labiano, F., García-Díez, E., de Diego, L. F., Serrano, A., Abad, A., Gayán, P., Adánez, J., & Ruíz, J. A. C. (2015b). Syngas/H<sub>2</sub> production from bioethanol in a continuous chemical-looping reforming prototype. *Fuel Processing Technology*, 137, 24–30. <https://doi.org/10.1016/J.FUPROC.2015.03.022>
- Guerrero-Caballero, J., Kane, T., Haidar, N., Jalowiecki-Duhamel, L., & Löfberg, A. (2019). Ni, Co, Fe supported on Ceria and Zr doped Ceria as oxygen carriers for chemical looping dry reforming of methane. *Catalysis Today*, 333, 251–258. <https://doi.org/10.1016/J.CATTOD.2018.11.064>
- Guo, L., Zhao, H., & Zheng, C. (2015). Synthesis Gas Generation by Chemical-Looping Reforming of Biomass with Natural Copper Ore as Oxygen Carrier. *Waste and Biomass Valorization*, 6(1), 81–89. <https://doi.org/10.1007/S12649-014-9328-1/FIGURES/8>
- Guo, M., Cheng, Z., Liu, Y., Qin, L., Goetze, J., Fan, J. A., & Fan, L. S. (2020). Cobalt doping modification for enhanced methane conversion at low temperature in chemical looping reforming systems. *Catalysis Today*, 350, 156–164. <https://doi.org/10.1016/J.CATTOD.2019.06.016>
- Hafizi, A., Rahimpour, M. R., & Hassanajili, S. (2016). High purity hydrogen production via sorption enhanced chemical looping reforming: Application of 22Fe<sub>2</sub>O<sub>3</sub>/MgAl<sub>2</sub>O<sub>4</sub> and 22Fe<sub>2</sub>O<sub>3</sub>/Al<sub>2</sub>O<sub>3</sub> as oxygen carriers and cerium promoted CaO as CO<sub>2</sub> sorbent. *Applied Energy*, 169, 629–641. <https://doi.org/10.1016/J.APENERGY.2016.02.068>
- Han, Y., Tian, M., Wang, C., Kang, Y., Kang, L., Su, Y., Huang, C., Zong, T., Lin, J., Hou, B., Pan, X., & Wang, X. (2022). Highly Active and Anticoke Ni/CeO<sub>2</sub> with Ultralow Ni Loading in Chemical Looping Dry Reforming via the Strong Metal–Support Interaction. 23, 29. <https://doi.org/10.1021/acssuschemeng.1c06079>
- Hassani Rad, S. J., Haghighi, M., Alizadeh Eslami, A., Rahmani, F., & Rahemi, N. (2016). Sol–gel vs. impregnation preparation of MgO and CeO<sub>2</sub> doped Ni/Al<sub>2</sub>O<sub>3</sub> nanocatalysts used in dry reforming of methane: Effect of process conditions, synthesis method and support composition. *International Journal of Hydrogen Energy*, 41(11), 5335–5350. <https://doi.org/10.1016/J.IJHYDENE.2016.02.002>
- Hossain, M. M., & de Lasa, H. I. (2008). Chemical-looping combustion (CLC) for inherent CO<sub>2</sub> separations—a review. *Chemical Engineering Science*, 63(18), 4433–4451. <https://doi.org/10.1016/J.CES.2008.05.028>



- Hu, G., Nicholas, N. J., Smith, K. H., Mumford, K. A., Kentish, S. E., & Stevens, G. W. (2016). Carbon dioxide absorption into promoted potassium carbonate solutions: A review. *International Journal of Greenhouse Gas Control*, 53, 28–40. <https://doi.org/10.1016/J.IJGGC.2016.07.020>
- Hu, J., Chen, S., & Xiang, W. (2021). Ni, Co and Cu-promoted iron-based oxygen carriers in methane-fueled chemical looping hydrogen generation process. *Fuel Processing Technology*, 221, 106917. <https://doi.org/10.1016/J.FUPROC.2021.106917>
- Hu, J., Zhang, T., Zhang, Q., Yan, X., Zhao, S., Dang, J., & Wang, W. (2021). Application of calcium oxide/ferric oxide composite oxygen carrier for corn straw chemical looping gasification. *Bioresource Technology*, 330, 125011. <https://doi.org/10.1016/J.BIORTECH.2021.125011>
- Hu, Z., Miao, Z., Wu, J., & Jiang, E. (2021). Nickel-iron modified natural ore oxygen carriers for chemical looping steam methane reforming to produce hydrogen. *International Journal of Hydrogen Energy*, 46(80), 39700–39718. <https://doi.org/10.1016/J.IJHYDENE.2021.09.242>
- Huang, J., Liu, W., Hu, W., Metcalfe, I., Yang, Y., & Liu, B. (2019). Phase interactions in Ni-Cu-Al<sub>2</sub>O<sub>3</sub> mixed oxide oxygen carriers for chemical looping applications. *Applied Energy*, 236, 635–647. <https://doi.org/10.1016/J.APENERGY.2018.12.029>
- Huang, J., Liu, W., Yang, Y., & Liu, B. (2018). High-Performance Ni-Fe Redox Catalysts for Selective CH<sub>4</sub> to Syngas Conversion via Chemical Looping. *ACS Catalysis*, 8(3), 1748–1756. [https://doi.org/10.1021/ACSCATAL.7B03964/ASSET/IMAGES/LARGE/CS-2017-03964E\\_0005.JPEG](https://doi.org/10.1021/ACSCATAL.7B03964/ASSET/IMAGES/LARGE/CS-2017-03964E_0005.JPEG)
- Huang, Z., Jiang, H., He, F., Chen, D., Wei, G., Zhao, K., Zheng, A., Feng, Y., Zhao, Z., & Li, H. (2016). Evaluation of multi-cycle performance of chemical looping dry reforming using CO<sub>2</sub> as an oxidant with Fe–Ni bimetallic oxides. *Journal of Energy Chemistry*, 25(1), 62–70. <https://doi.org/10.1016/J.JECHEM.2015.10.008>
- Iglesias, I., Baronetti, G., & Mariño, F. (2017). Ni/Ce<sub>0.95</sub>M<sub>0.05</sub>O<sub>2-d</sub> (M = Zr, Pr, La) for methane steam reforming at mild conditions. *International Journal of Hydrogen Energy*, 42(50), 29735–29744. <https://doi.org/10.1016/J.IJHYDENE.2017.09.176>
- Iliuta, M. C. (2013). *Biosyngas Production in an Integrated Aqueous-Phase Glycerol Reforming/Chemical Looping Combustion Process*. <https://doi.org/10.1021/ie402114k>
- Imtiaz, Q., Yüzbaşı, N. S., Abdala, P. M., Kierzkowska, A. M., van Beek, W., Broda, M., & Müller, C. R. (2015). Development of MgAl<sub>2</sub>O<sub>4</sub>-stabilized, Cu-doped, Fe<sub>2</sub>O<sub>3</sub>-based oxygen carriers for thermochemical water-splitting. *Journal of Materials Chemistry A*, 4(1), 113–123. <https://doi.org/10.1039/C5TA06753G>
- Iriondo, A., Barrio, V. L., Cambra, J. F., Arias, P. L., Güemez, M. B., Navarro, R. M., Sánchez-Sánchez, M. C., & Fierro, J. L. G. (2008). Hydrogen production from glycerol over nickel catalysts supported on Al<sub>2</sub>O<sub>3</sub> modified by Mg, Zr, Ce or La. *Topics in Catalysis*, 49(1–2), 46–58. <https://doi.org/10.1007/S11244-008-9060-9/TABLES/9>

- Isarapakdeetham, S., Kim-Lohsoontorn, P., Wongsakulphasatch, S., Kiatkittipong, W., Laosiripojana, N., Gong, J., & Assabumrungrat, S. (2020). Hydrogen production via chemical looping steam reforming of ethanol by Ni-based oxygen carriers supported on CeO<sub>2</sub> and La<sub>2</sub>O<sub>3</sub> promoted Al<sub>2</sub>O<sub>3</sub>. *International Journal of Hydrogen Energy*, 45(3), 1477–1491. <https://doi.org/10.1016/J.IJHYDENE.2019.11.077>
- Jang, J. T., Yoon, K. J., Bae, J. W., & Han, G. Y. (2014). Cyclic production of syngas and hydrogen through methane-reforming and water-splitting by using ceria–zirconia solid solutions in a solar volumetric receiver–reactor. *Solar Energy*, 109(1), 70–81. <https://doi.org/10.1016/J.SOLENER.2014.08.024>
- Jerndal, E., Mattisson, T., & Lyngfelt, A. (2006). Thermal Analysis of Chemical-Looping Combustion. *Chemical Engineering Research and Design*, 84(9), 795–806. <https://doi.org/10.1205/CHERD05020>
- Ji, M., & Wang, J. (2021). Review and comparison of various hydrogen production methods based on costs and life cycle impact assessment indicators. *International Journal of Hydrogen Energy*, 46(78), 38612–38635. <https://doi.org/10.1016/J.IJHYDENE.2021.09.142>
- Jiang, B., Dou, B., Song, Y., Zhang, C., Du, B., Chen, H., Wang, C., & Xu, Y. (2015). Hydrogen production from chemical looping steam reforming of glycerol by Ni-based oxygen carrier in a fixed-bed reactor. *Chemical Engineering Journal*, 280, 459–467. <https://doi.org/10.1016/J.CEJ.2015.05.120>
- Jiang, B., Dou, B., Wang, K., Zhang, C., Song, Y., Chen, H., & Xu, Y. (2016). Hydrogen production by chemical looping steam reforming of ethanol using NiO/montmorillonite oxygen carriers in a fixed-bed reactor. *Chemical Engineering Journal*, 298, 96–106. <https://doi.org/10.1016/J.CEJ.2016.04.027>
- Jiang, B., Li, L., Bian, Z., Li, Z., Othman, M., Sun, Z., Tang, D., Kawi, S., & Dou, B. (2018). Hydrogen generation from chemical looping reforming of glycerol by Ce-doped nickel phyllosilicate nanotube oxygen carriers. *Fuel*, 222, 185–192. <https://doi.org/10.1016/J.FUEL.2018.02.096>
- Jiang, B., Li, L., Bian, Z., Li, Z., Sun, Y., Sun, Z., Tang, D., Kawi, S., Dou, B., & Goula, M. A. (2018). Chemical looping glycerol reforming for hydrogen production by Ni@ZrO<sub>2</sub> nanocomposite oxygen carriers. *International Journal of Hydrogen Energy*, 43(29), 13200–13211. <https://doi.org/10.1016/J.IJHYDENE.2018.05.065>
- Jiang, B., Li, L., Zhang, Q., Ma, J., Zhang, H., Bai, J., Bian, Z., Dou, B., Kawi, S., & Tang, D. (2020). Chemical Looping Reforming of Glycerol for Continuous H<sub>2</sub> Production by Moving-Bed Reactors: Simulation and Experiment. *Energy and Fuels*, 34(2), 1841–1850. [https://doi.org/10.1021/ACS.ENERGYFUELS.9B03728/ASSET/IMAGES/LARGE/EF9B03728\\_0010.JPEG](https://doi.org/10.1021/ACS.ENERGYFUELS.9B03728/ASSET/IMAGES/LARGE/EF9B03728_0010.JPEG)
- Jiao, Y., He, Z., Wang, J., & Chen, Y. (2017). n-decane steam reforming for hydrogen production over mono- and bi-metallic Co-Ni/Ce-Al<sub>2</sub>O<sub>3</sub> catalysts: Structure-activity correlations. *Energy Conversion and Management*, 148, 954–962. <https://doi.org/10.1016/J.ENCONMAN.2017.06.065>

- Johansson, M., Mattisson, T., & Lyngfelt, A. (2006). Investigation of  $\text{Mn}_3\text{O}_4$  With Stabilized  $\text{ZrO}_2$  for Chemical-Looping Combustion. *Chemical Engineering Research and Design*, 84(9), 807–818. <https://doi.org/10.1205/CHERD.05206>
- Johansson, M., Mattisson, T., Lyngfelt, A., & Abad, A. (2008). Using continuous and pulse experiments to compare two promising nickel-based oxygen carriers for use in chemical-looping technologies. *Fuel*, 87(6), 988–1001. <https://doi.org/10.1016/J.FUEL.2007.08.010>
- Kang, D., Lim, H. S., Lee, M., & Lee, J. W. (2018). Syngas production on a Ni-enhanced  $\text{Fe}_2\text{O}_3/\text{Al}_2\text{O}_3$  oxygen carrier via chemical looping partial oxidation with dry reforming of methane. *Applied Energy*, 211, 174–186. <https://doi.org/10.1016/J.APENERGY.2017.11.018>
- Kang, Y., Tian, M., Huang, C., Lin, J., Hou, B., Pan, X., Li, L., Rykov, A. I., Wang, J., & Wang, X. (2019). Improving Syngas Selectivity of  $\text{Fe}_2\text{O}_3/\text{Al}_2\text{O}_3$  with Yttrium Modification in Chemical Looping Methane Conversion. *ACS Catalysis*, 9(9), 8373–8382. [https://doi.org/10.1021/ACSCATAL.9B02730/ASSET/IMAGES/LARGE/CS9B02730\\_0008.JPEG](https://doi.org/10.1021/ACSCATAL.9B02730/ASSET/IMAGES/LARGE/CS9B02730_0008.JPEG)
- Keller, M., Fung, J., Leion, H., & Mattisson, T. (2016). Cu-impregnated alumina/silica bed materials for Chemical Looping Reforming of biomass gasification gas. *Fuel*, 180, 448–456. <https://doi.org/10.1016/J.FUEL.2016.04.024>
- Khajenoori, M., Rezaei, M., & Meshkani, F. (2015). Dry reforming over  $\text{CeO}_2$ -promoted Ni/MgO nano-catalyst: Effect of Ni loading and  $\text{CH}_4/\text{CO}_2$  molar ratio. *Journal of Industrial and Engineering Chemistry*, 21, 717–722. <https://doi.org/10.1016/J.JIEC.2014.03.043>
- Khzouz, M., Wood, J., Pollet, B., & Bujalski, W. (2013). Characterization and activity test of commercial Ni/ $\text{Al}_2\text{O}_3$ , Cu/ $\text{ZnO}/\text{Al}_2\text{O}_3$  and prepared Ni–Cu/ $\text{Al}_2\text{O}_3$  catalysts for hydrogen production from methane and methanol fuels. *International Journal of Hydrogen Energy*, 38(3), 1664–1675. <https://doi.org/10.1016/J.IJHYDENE.2012.07.026>
- Lee, D., Nam, H., Kim, H., Hwang, B., Baek, J. I., & Ryu, H. J. (2021). Experimental screening of oxygen carrier for a pressurized chemical looping combustion. *Fuel Processing Technology*, 218, 106860. <https://doi.org/10.1016/J.FUPROC.2021.106860>
- Li, D., Li, K., Xu, R., Zhu, X., Wei, Y., Tian, D., Cheng, X., & Wang, H. (2019). Enhanced  $\text{CH}_4$  and CO Oxidation over  $\text{Ce}_1\text{-xFe}_x\text{O}_2$ -Hybrid Catalysts by Tuning the Lattice Distortion and the State of Surface Iron Species. *ACS Applied Materials and Interfaces*, 11(21), 19227–19241. [https://doi.org/10.1021/ACSAMI.9B05409/ASSET/IMAGES/LARGE/AM-2019-05409J\\_0013.JPEG](https://doi.org/10.1021/ACSAMI.9B05409/ASSET/IMAGES/LARGE/AM-2019-05409J_0013.JPEG)
- Li, D., Xu, R., Jia, Y., Ning, P., & Li, K. (2019). Controlled synthesis of  $\alpha\text{-Fe}_2\text{O}_3$  hollows from  $\beta\text{-FeOOH}$  rods. *Chemical Physics Letters*, 731, 136623. <https://doi.org/10.1016/J.CPLETT.2019.136623>

- Li, D., Xu, S., Song, K., Chen, C., Zhan, Y., & Jiang, L. (2018). Hydrotalcite-derived Co/Mg(Al)O as a stable and coke-resistant catalyst for low-temperature carbon dioxide reforming of methane. *Applied Catalysis A: General*, 552, 21–29. <https://doi.org/10.1016/J.APCATA.2017.12.022>
- Li, L., Jiang, B., Tang, D., Zheng, Z., & Zhao, C. (2018). Hydrogen Production from Chemical Looping Reforming of Ethanol Using Ni/CeO<sub>2</sub> Nanorod Oxygen Carrier. *Catalysts* 2018, Vol. 8, Page 257, 8(7), 257. <https://doi.org/10.3390/CATAL8070257>
- Li, L., Song, Y., Jiang, B., Wang, K., & Zhang, Q. (2017). A novel oxygen carrier for chemical looping reforming: LaNiO<sub>3</sub> perovskite supported on montmorillonite. *Energy*, 131, 58–66. <https://doi.org/10.1016/J.ENERGY.2017.05.030>
- Li, T., Wu, Q., Wang, W., Xiao, Y. P., Liu, C., & Yang, F. (2020). Solid-solid reaction of CuFe<sub>2</sub>O<sub>4</sub> with C in chemical looping system: A comprehensive study. *Fuel*, 267, 117163. <https://doi.org/10.1016/J.FUEL.2020.117163>
- Lind, F., Israelsson, M., Seemann, M., & Thunman, H. (2012). Manganese oxide as catalyst for tar cleaning of biomass-derived gas. *Biomass Conversion and Biorefinery*, 2(2), 133–140. <https://doi.org/10.1007/S13399-012-0042-6/FIGURES/5>
- Long, Y., Li, K., Gu, Z., Zhu, X., Wei, Y., Lu, C., Lin, S., Yang, K., Cheng, X., Tian, D., He, F., & Wang, H. (2020). Ce-Fe-Zr-O/MgO coated monolithic oxygen carriers for chemical looping reforming of methane to co-produce syngas and H<sub>2</sub>. *Chemical Engineering Journal*, 388, 124190. <https://doi.org/10.1016/J.CEJ.2020.124190>
- López Ortiz, A., Meléndez Zaragoza, M., & Collins-Martínez, V. (2015). Thermodynamic analysis of the ethanol chemical looping autothermal reforming with CO<sub>2</sub> capture. *International Journal of Hydrogen Energy*, 40(48), 17180–17191. <https://doi.org/10.1016/J.IJHYDENE.2015.08.035>
- Lu, C., Xu, R., Muhammad, I. Khan, Zhu, X., Wei, Y., Qi, X., & Li, K. (2021). Thermodynamic evolution of magnetite oxygen carrier via chemical looping reforming of methane. *Journal of Natural Gas Science and Engineering*, 85. <https://doi.org/10.1016/J.JNGSE.2020.103704>
- Luo, C., Dou, B., Zhang, H., Zhao, L., Zeng, P., Gao, D., Wang, Y., Chen, H., & Xu, Y. (2022). Hydrogen and syngas co-production by coupling of chemical looping water splitting and glycerol oxidation reforming using Ce–Ni modified Fe-based oxygen carriers. *Journal of Cleaner Production*, 335, 130299. <https://doi.org/10.1016/J.JCLEPRO.2021.130299>
- Ma, Z., Zhang, S., & Lu, Y. (2020). Activation mechanism of Fe<sub>2</sub>O<sub>3</sub>-Al<sub>2</sub>O<sub>3</sub> oxygen carrier in chemical looping combustion. *Energy and Fuels*, 34(12), 16350–16355. [https://doi.org/10.1021/ACS.ENERGYFUELS.0C02967/ASSET/IMAGES/LARGE/EF0C02967\\_0008.JPEG](https://doi.org/10.1021/ACS.ENERGYFUELS.0C02967/ASSET/IMAGES/LARGE/EF0C02967_0008.JPEG)
- Martini, M., Druiff, M., van Sint Annaland, M., & Gallucci, F. (2021). Experimental demonstration of the Ca-Cu looping process. *Chemical Engineering Journal*, 418, 129505. <https://doi.org/10.1016/J.CEJ.2021.129505>

- Martini, M., Jain, S., Gallucci, F., & van Sint Annaland, M. (2021). Model validation of the Ca-Cu looping process. *Chemical Engineering Journal*, 410, 128351. <https://doi.org/10.1016/J.CEJ.2020.128351>
- Masoudi Soltani, S., Lahiri, A., Bahzad, H., Clough, P., Gorbounov, M., & Yan, Y. (2021). Sorption-enhanced Steam Methane Reforming for Combined CO<sub>2</sub> Capture and Hydrogen Production: A State-of-the-Art Review. *Carbon Capture Science & Technology*, 1, 100003. <https://doi.org/10.1016/J.CCST.2021.100003>
- Medrano, J. A., Potdar, I., Melendez, J., Spallina, V., Pacheco-Tanaka, D. A., van Sint Annaland, M., & Gallucci, F. (2018). The membrane-assisted chemical looping reforming concept for efficient H<sub>2</sub> production with inherent CO<sub>2</sub> capture: Experimental demonstration and model validation. *Applied Energy*, 215, 75–86. <https://doi.org/10.1016/J.APENERGY.2018.01.087>
- Medrano, J. A., Spallina, V., van Sint Annaland, M., & Gallucci, F. (2014). Thermodynamic analysis of a membrane-assisted chemical looping reforming reactor concept for combined H<sub>2</sub> production and CO<sub>2</sub> capture. *International Journal of Hydrogen Energy*, 39(9), 4725–4738. <https://doi.org/10.1016/J.IJHYDENE.2013.11.126>
- Mendoza-Nieto, J. A., Duan, Y., & Pfeiffer, H. (2018). Alkaline zirconates as effective materials for hydrogen production through consecutive carbon dioxide capture and conversion in methane dry reforming. *Applied Catalysis B: Environmental*, 238, 576–585. <https://doi.org/10.1016/J.APCATB.2018.07.065>
- Meshksar, M., Daneshmand-Jahromi, S., & Rahimpour, M. R. (2017). Synthesis and characterization of cerium promoted Ni/SBA-16 oxygen carrier in cyclic chemical looping steam methane reforming. *Journal of the Taiwan Institute of Chemical Engineers*, 76, 73–82. <https://doi.org/10.1016/J.JTICE.2017.04.012>
- Nadgouda, S. G., Guo, M., Tong, A., & Fan, L. S. (2019). High purity syngas and hydrogen coproduction using copper-iron oxygen carriers in chemical looping reforming process. *Applied Energy*, 235, 1415–1426. <https://doi.org/10.1016/J.APENERGY.2018.11.051>
- Nandy, A., Loha, C., Gu, S., Sarkar, P., Karmakar, M. K., & Chatterjee, P. K. (2016). Present status and overview of Chemical Looping Combustion technology. *Renewable and Sustainable Energy Reviews*, 59, 597–619. <https://doi.org/10.1016/J.RSER.2016.01.003>
- Nazari, M., Soltanieh, M., Heydarinasab, A., & Maddah, B. (2021). Synthesis of a new self-supported Mgy(CuxNi0.6-xMn0.4)1-yFe2O4 oxygen carrier for chemical looping steam methane reforming process. *International Journal of Hydrogen Energy*, 46(37), 19397–19420. <https://doi.org/10.1016/J.IJHYDENE.2021.03.081>
- Nazir, S. M., Morgado, J. F., Bolland, O., Quinta-Ferreira, R., & Amini, S. (2018). Techno-economic assessment of chemical looping reforming of natural gas for hydrogen production and power generation with integrated CO<sub>2</sub> capture. *International Journal of Greenhouse Gas Control*, 78, 7–20. <https://doi.org/10.1016/J.IJGGC.2018.07.022>

- Neal, L., Shafieifarhood, A., & Li, F. (2015). Effect of core and shell compositions on MeOx@LaySr1- $\gamma$ FeO3 core-shell redox catalysts for chemical looping reforming of methane. *Applied Energy*, 157, 391–398. <https://doi.org/10.1016/J.APENERGY.2015.06.028>
- Ni, Y., Wang, C., Chen, Y., Cai, X., Dou, B., Chen, H., Xu, Y., Jiang, B., & Wang, K. (2017). High purity hydrogen production from sorption enhanced chemical looping glycerol reforming: Application of NiO-based oxygen transfer materials and potassium promoted Li2ZrO3 as CO2 sorbent. *Applied Thermal Engineering*, 124, 454–465. <https://doi.org/10.1016/J.APPLTHERMALENG.2017.06.003>
- Nieva, M. A., Villaverde, M. M., Monzón, A., Garetto, T. F., & Marchi, A. J. (2014). Steam-methane reforming at low temperature on nickel-based catalysts. *Chemical Engineering Journal*, 235, 158–166. <https://doi.org/10.1016/J.CEJ.2013.09.030>
- Nikoo, M. K., & Amin, N. A. S. (2011). Thermodynamic analysis of carbon dioxide reforming of methane in view of solid carbon formation. *Fuel Processing Technology*, 92(3), 678–691. <https://doi.org/10.1016/J.FUPROC.2010.11.027>
- Nimmas, T., Wongsakulphasatch, S., Kui Cheng, C., & Assabumrungrat, S. (2020). Bi-metallic CuO-NiO based multifunctional material for hydrogen production from sorption-enhanced chemical looping autothermal reforming of ethanol. *Chemical Engineering Journal*, 398, 125543. <https://doi.org/10.1016/J.CEJ.2020.125543>
- Osman, M., Khan, M. N., Zaabout, A., Cloete, S., & Amini, S. (2021). Review of pressurized chemical looping processes for power generation and chemical production with integrated CO2 capture. *Fuel Processing Technology*, 214, 106684. <https://doi.org/10.1016/J.FUPROC.2020.106684>
- Ozbilen, A., Dincer, I., & Rosen, M. A. (2013). Comparative environmental impact and efficiency assessment of selected hydrogen production methods. *Environmental Impact Assessment Review*, 42, 1–9. <https://doi.org/10.1016/J.EIAR.2013.03.003>
- Pantaleo, G., la Parola, V., Deganello, F., Calatizzo, P., Bal, R., & Venezia, A. M. (2015). Synthesis and support composition effects on CH4 partial oxidation over Ni-CeLa oxides. *Applied Catalysis B: Environmental*, 164, 135–143. <https://doi.org/10.1016/J.APCATB.2014.09.011>
- Papageridis, K. N., Siakavelas, G., Charisiou, N. D., Avraam, D. G., Tzounis, L., Kousi, K., & Goula, M. A. (2016). Comparative study of Ni, Co, Cu supported on  $\gamma$ -alumina catalysts for hydrogen production via the glycerol steam reforming reaction. *Fuel Processing Technology*, 152, 156–175. <https://doi.org/10.1016/J.FUPROC.2016.06.024>
- Papageridis, K. N., Siakavelas, G., Charisiou, N. D., & Goula, M. A. (n.d.). *Effect of the active metal supported on SiO2 to the selective hydrogen production on the glycerol steam reforming reaction.*

- Patcharavorachot, Y., Chatrattanawet, N., Arpornwichanop, A., & Assabumrungrat, S. (2019). Optimization of hydrogen production from three reforming approaches of glycerol via using supercritical water with in situ CO<sub>2</sub> separation. *International Journal of Hydrogen Energy*, 44(4), 2128–2140. <https://doi.org/10.1016/J.IJHYDENE.2018.07.053>
- Patil, C. S., van Sint Annaland, M., & Kuipers, J. A. M. (2007). Fluidised bed membrane reactor for ultrapure hydrogen production via methane steam reforming: Experimental demonstration and model validation. *Chemical Engineering Science*, 62(11), 2989–3007. <https://doi.org/10.1016/J.CES.2007.02.022>
- Porrizzo, R., White, G., & Ocone, R. (2014). Aspen Plus simulations of fluidised beds for chemical looping combustion. *Fuel*, 136, 46–56. <https://doi.org/10.1016/J.FUEL.2014.06.053>
- Qin, L., Guo, M., Liu, Y., Cheng, Z., Fan, J. A., & Fan, L. S. (2018). Enhanced methane conversion in chemical looping partial oxidation systems using a copper doping modification. *Applied Catalysis B: Environmental*, 235, 143–149. <https://doi.org/10.1016/J.APCATB.2018.04.072>
- Qingli, X., Zhengdong, Z., Kai, H., Shanzhi, X., Chuang, M., Chenge, C., Huan, Y., Yang, Y., & Yongjie, Y. (2021). Ni supported on MgO modified attapulgite as catalysts for hydrogen production from glycerol steam reforming. *International Journal of Hydrogen Energy*, 46(54), 27380–27393. <https://doi.org/10.1016/J.IJHYDENE.2021.06.028>
- Rahbar Shamskar, F., Meshkani, F., & Rezaei, M. (2017). Preparation and characterization of ultrasound-assisted co-precipitated nanocrystalline La-, Ce-, Zr –promoted Ni-Al<sub>2</sub>O<sub>3</sub> catalysts for dry reforming reaction. *Journal of CO<sub>2</sub> Utilization*, 22, 124–134. <https://doi.org/10.1016/J.JCOU.2017.09.014>
- Roslan, N. A., Abidin, S. Z., Ideris, A., & Vo, D. V. N. (2020). A review on glycerol reforming processes over Ni-based catalyst for hydrogen and syngas productions. *International Journal of Hydrogen Energy*, 45(36), 18466–18489. <https://doi.org/10.1016/J.IJHYDENE.2019.08.211>
- Rydén, M., Lyngfelt, A., & Mattisson, T. (2008). Chemical-looping combustion and chemical-looping reforming in a circulating fluidized-bed reactor using Ni-based oxygen carriers. *Energy and Fuels*, 22(4), 2585–2597. [https://doi.org/10.1021/EF800065M/ASSET/IMAGES/LARGE/EF-2008-00065M\\_0001.JPEG](https://doi.org/10.1021/EF800065M/ASSET/IMAGES/LARGE/EF-2008-00065M_0001.JPEG)
- Rydén, M., Lyngfelt, A., & Mattisson, T. (2011). CaMn<sub>0.875</sub>Ti<sub>0.125</sub>O<sub>3</sub> as oxygen carrier for chemical-looping combustion with oxygen uncoupling (CLOU)—Experiments in a continuously operating fluidized-bed reactor system. *International Journal of Greenhouse Gas Control*, 5(2), 356–366. <https://doi.org/10.1016/J.IJGGC.2010.08.004>
- Sastre, D., Galván, C. Á., Pizarro, P., & Coronado, J. M. (2022). Enhanced performance of CH<sub>4</sub> dry reforming over La<sub>0.9</sub>Sr<sub>0.1</sub>FeO<sub>3</sub>/YSZ under chemical looping conditions. *Fuel*, 309, 122122. <https://doi.org/10.1016/J.FUEL.2021.122122>

- Sastre, D., Serrano, D. P., Pizarro, P., & Coronado, J. M. (2019). Chemical insights on the activity of  $\text{La}_{1-x}\text{Sr}_x\text{FeO}_3$  perovskites for chemical looping reforming of methane coupled with  $\text{CO}_2$ -splitting. *Journal of CO<sub>2</sub> Utilization*, 31, 16–26. <https://doi.org/10.1016/J.JCOU.2019.02.013>
- Saupsor, J., Kasempremchit, N., Bumroongsakulsawat, P., Kim-Lohsoontorn, P., Wongsakulphasatch, S., Kiatkittipong, W., Laosiripojana, N., Gong, J., & Assabumrungrat, S. (2020). Performance comparison among different multifunctional reactors operated under energy self-sufficiency for sustainable hydrogen production from ethanol. *International Journal of Hydrogen Energy*, 45(36), 18309–18320. <https://doi.org/10.1016/J.IJHYDENE.2019.03.090>
- Saupsor, J., Pei, C., Li, H., Wongsakulphasatch, S., Kim-Lohsoontorn, P., Ratchahat, S., Kiatkittipong, W., Assabumrungrat, S., & Gong, J. (2021). Bifunctional Catalyst  $\text{NiFe-MgAl}$  for Hydrogen Production from Chemical Looping Ethanol Reforming. *Energy and Fuels*, 35(14), 11580–11592. [https://doi.org/10.1021/ACS.ENERGYFUELS.1C01253/ASSET/IMAGES/LARGE/EF1C01253\\_0015.JPEG](https://doi.org/10.1021/ACS.ENERGYFUELS.1C01253/ASSET/IMAGES/LARGE/EF1C01253_0015.JPEG)
- Shah, V., Cheng, Z., Baser, D. S., Fan, J. A., & Fan, L. S. (2021). Highly Selective Production of Syngas from Chemical Looping Reforming of Methane with  $\text{CO}_2$  Utilization on  $\text{MgO}$ -supported Calcium Ferrite Redox Materials. *Applied Energy*, 282, 116111. <https://doi.org/10.1016/J.APENERGY.2020.116111>
- Siriwardane, R., Tian, H., & Fisher, J. (2015). Production of pure hydrogen and synthesis gas with  $\text{Cu-Fe}$  oxygen carriers using combined processes of chemical looping combustion and methane decomposition/reforming. *International Journal of Hydrogen Energy*, 40(4), 1698–1708. <https://doi.org/10.1016/J.IJHYDENE.2014.11.090>
- Solunke, R. D., & Vesper, G. (2010). Hydrogen production via chemical looping steam reforming in a periodically operated fixed-bed reactor. *Industrial and Engineering Chemistry Research*, 49(21), 11037–11044. [https://doi.org/10.1021/IE100432J/ASSET/IMAGES/LARGE/IE-2010-00432J\\_0006.JPEG](https://doi.org/10.1021/IE100432J/ASSET/IMAGES/LARGE/IE-2010-00432J_0006.JPEG)
- Spallina, V., Gallucci, F., Romano, M. C., & van Sint Annaland, M. (2016). Pre-combustion packed bed chemical looping (PCCL) technology for efficient  $\text{H}_2$ -rich gas production processes. *Chemical Engineering Journal*, 294, 478–494. <https://doi.org/10.1016/J.CEJ.2016.03.011>
- Spallina, V., Marinello, B., Gallucci, F., Romano, M. C., & van Sint Annaland, M. (2017). Chemical looping reforming in packed-bed reactors: Modelling, experimental validation and large-scale reactor design. *Fuel Processing Technology*, 156, 156–170. <https://doi.org/10.1016/J.FUPROC.2016.10.014>
- Spallina, V., Motamedi, G., Gallucci, F., & van Sint Annaland, M. (2019). Techno-economic assessment of an integrated high pressure chemical-looping process with packed-bed reactors in large scale hydrogen and methanol production. *International Journal of Greenhouse Gas Control*, 88, 71–84. <https://doi.org/10.1016/J.IJGGC.2019.05.026>
- Spallina, V., Pandolfo, D., Battistella, A., Romano, M. C., van Sint Annaland, M., & Gallucci, F. (2016). Techno-economic assessment of membrane assisted fluidized bed reactors for pure  $\text{H}_2$  production with  $\text{CO}_2$



capture. *Energy Conversion and Management*, 120, 257–273.

<https://doi.org/10.1016/J.ENCONMAN.2016.04.073>

Suero, S. R., Cano, B. L., Álvarez-Murillo, A., Al-Kassir, A., & Yusaf, T. (2015). Glycerin, a Biodiesel By-Product with Potentiality to Produce Hydrogen by Steam Gasification. *Energies* 2015, Vol. 8, Pages 12765-12775, 8(11), 12765–12775. <https://doi.org/10.3390/EN81112339>

Sun, Y., Li, J., & Li, H. (2022). Core-shell-like Fe<sub>2</sub>O<sub>3</sub>/MgO oxygen carriers matched with fluidized bed reactor for chemical looping reforming. *Chemical Engineering Journal*, 431, 134173. <https://doi.org/10.1016/J.CEJ.2021.134173>

Sun, Z., Lu, D. Y., Symonds, R. T., & Hughes, R. W. (2020). Chemical looping reforming of CH<sub>4</sub> in the presence of CO<sub>2</sub> using ilmenite ore and NiO-modified ilmenite ore oxygen carriers. *Chemical Engineering Journal*, 401, 123481. <https://doi.org/10.1016/J.CEJ.2019.123481>

Svoboda, K., Siewiorek, A., Baxter, D., Rogut, J., & Pohořelý, M. (2008). Thermodynamic possibilities and constraints for pure hydrogen production by a nickel and cobalt-based chemical looping process at lower temperatures. *Energy Conversion and Management*, 49(2), 221–231. <https://doi.org/10.1016/J.ENCONMAN.2007.06.036>

Tang, M., Xu, L., & Fan, M. (2015). Progress in oxygen carrier development of methane-based chemical-looping reforming: A review. *Applied Energy*, 151, 143–156. <https://doi.org/10.1016/J.APENERGY.2015.04.017>

Tavanarad, M., Rezaei, M., & Meshkani, F. (2021). Preparation and evaluation of Ni/γ-Al<sub>2</sub>O<sub>3</sub> catalysts promoted by alkaline earth metals in glycerol reforming with carbon dioxide. *International Journal of Hydrogen Energy*, 46(49), 24991–25003. <https://doi.org/10.1016/J.IJHYDENE.2021.05.033>

Teh, L. P., Setiabudi, H. D., Timmiati, S. N., Aziz, M. A. A., Annuar, N. H. R., & Ruslan, N. N. (2021). Recent progress in ceria-based catalysts for the dry reforming of methane: A review. *Chemical Engineering Science*, 242, 116606. <https://doi.org/10.1016/J.CES.2021.116606>

Tian, X., Su, M., & Zhao, H. (2020). Kinetics of redox reactions of CuO@TiO<sub>2</sub>–Al<sub>2</sub>O<sub>3</sub> for chemical looping combustion and chemical looping with oxygen uncoupling. *Combustion and Flame*, 213, 255–267. <https://doi.org/10.1016/J.COMBUSTFLAME.2019.11.044>

Trevisanut, C., Mari, M., Millet, J. M., & Cavani, F. (2015). Chemical-loop reforming of ethanol over metal ferrites: An analysis of structural features affecting reactivity. *International Journal of Hydrogen Energy*, 40(15), 5264–5271. <https://doi.org/10.1016/J.IJHYDENE.2015.01.054>

Usman, M., Wan Daud, W. M. A., & Abbas, H. F. (2015). Dry reforming of methane: Influence of process parameters—A review. *Renewable and Sustainable Energy Reviews*, 45, 710–744. <https://doi.org/10.1016/J.RSER.2015.02.026>

- van Renssen, S. (2020). The hydrogen solution? *Nature Climate Change* 2020 10:9, 10(9), 799–801.  
<https://doi.org/10.1038/s41558-020-0891-0>
- Vizcaíno, A. J., Arena, P., Baronetti, G., Carrero, A., Calles, J. A., Laborde, M. A., & Amadeo, N. (2008). Ethanol steam reforming on Ni/Al<sub>2</sub>O<sub>3</sub> catalysts: Effect of Mg addition. *International Journal of Hydrogen Energy*, 33(13), 3489–3492. <https://doi.org/10.1016/J.IJHYDENE.2007.12.012>
- Vos, Y. de, Jacobs, M., Voort, P. van der, Driessche, I. van, Snijkers, F., & Verberckmoes, A. (2020a). Development of Stable Oxygen Carrier Materials for Chemical Looping Processes—A Review. *Catalysts* 2020, Vol. 10, Page 926, 10(8), 926. <https://doi.org/10.3390/CATAL10080926>
- Vos, Y. de, Jacobs, M., Voort, P. van der, Driessche, I. van, Snijkers, F., & Verberckmoes, A. (2020b). Development of Stable Oxygen Carrier Materials for Chemical Looping Processes—A Review. *Catalysts* 2020, Vol. 10, Page 926, 10(8), 926. <https://doi.org/10.3390/CATAL10080926>
- Wang, C., Dou, B., Chen, H., Song, Y., Xu, Y., Du, X., Zhang, L., Luo, T., & Tan, C. (2013). Renewable hydrogen production from steam reforming of glycerol by Ni–Cu–Al, Ni–Cu–Mg, Ni–Mg catalysts. *International Journal of Hydrogen Energy*, 38(9), 3562–3571. <https://doi.org/10.1016/J.IJHYDENE.2013.01.042>
- Wang, K., Dou, B., Jiang, B., Song, Y., Zhang, C., Zhang, Q., Chen, H., & Xu, Y. (2016). Renewable hydrogen production from chemical looping steam reforming of ethanol using xCeNi/SBA-15 oxygen carriers in a fixed-bed reactor. *International Journal of Hydrogen Energy*, 41(30), 12899–12909.  
<https://doi.org/10.1016/J.IJHYDENE.2016.05.100>
- Wang, K., Dou, B., Jiang, B., Zhang, Q., Li, M., Chen, H., & Xu, Y. (2016). Effect of support on hydrogen production from chemical looping steam reforming of ethanol over Ni-based oxygen carriers. *International Journal of Hydrogen Energy*, 41(39), 17334–17347.  
<https://doi.org/10.1016/J.IJHYDENE.2016.07.261>
- Wang, P., Means, N., Shekhawat, D., Berry, D., & Massoudi, M. (2015). Chemical-Looping Combustion and Gasification of Coals and Oxygen Carrier Development: A Brief Review. *Energies* 2015, Vol. 8, Pages 10605–10635, 8(10), 10605–10635. <https://doi.org/10.3390/EN81010605>
- Wang, W., Fan, L., & Wang, G. (2017). Study on chemical looping reforming of ethanol (CLRE) for hydrogen production using NiMn<sub>2</sub>O<sub>4</sub> spinel as oxygen carrier. *Journal of the Energy Institute*, 90(6), 884–892.  
<https://doi.org/10.1016/J.JOEI.2016.08.006>
- Wang, X., Li, M., Wang, M., Wang, H., Li, S., Wang, S., & Ma, X. (2009). Thermodynamic analysis of glycerol dry reforming for hydrogen and synthesis gas production. *Fuel*, 88(11), 2148–2153.  
<https://doi.org/10.1016/J.FUEL.2009.01.015>

- Wang, Y., Zheng, Y., Wang, Y., Li, K., Wang, Y., Jiang, L., Zhu, X., Wei, Y., & Wang, H. (2019). Syngas production modified by oxygen vacancies over CeO<sub>2</sub>-ZrO<sub>2</sub>-CuO oxygen carrier via chemical looping reforming of methane. *Applied Surface Science*, 481, 151–160. <https://doi.org/10.1016/J.APSUSC.2019.03.050>
- Wang, Z., Zhu, M., He, T., Zhang, J., Wu, J., Tian, H., & Wu, J. (2018). Chemical looping reforming of toluene as a biomass tar model compound over two types of oxygen carriers: 2CuO-2NiO/Al<sub>2</sub>O<sub>3</sub> and CaFe<sub>2</sub>O<sub>4</sub>. *Fuel*, 222, 375–384. <https://doi.org/10.1016/J.FUEL.2018.02.164>
- Wassie, S. A., Gallucci, F., Zaabout, A., Cloete, S., Amini, S., & van Sint Annaland, M. (2017). Hydrogen production with integrated CO<sub>2</sub> capture in a novel gas switching reforming reactor: Proof-of-concept. *International Journal of Hydrogen Energy*, 42(21), 14367–14379. <https://doi.org/10.1016/J.IJHYDENE.2017.04.227>
- Wei, G., Huang, J., Fan, Y., Huang, Z., Zheng, A., He, F., Meng, J., Zhang, D., Zhao, K., Zhao, Z., & Li, H. (2019). Chemical looping reforming of biomass based pyrolysis gas coupling with chemical looping hydrogen by using Fe/Ni/Al oxygen carriers derived from LDH precursors. *Energy Conversion and Management*, 179, 304–313. <https://doi.org/10.1016/J.ENCONMAN.2018.10.065>
- Wei, Y., Wang, H., He, F., Ao, X., & Zhang, C. (2007). CeO<sub>2</sub> as the Oxygen Carrier for Partial Oxidation of Methane to Synthesis Gas in Molten Salts: Thermodynamic Analysis and Experimental Investigation. *Journal of Natural Gas Chemistry*, 16(1), 6–11. [https://doi.org/10.1016/S1003-9953\(07\)60018-8](https://doi.org/10.1016/S1003-9953(07)60018-8)
- Wu, G., Zhang, C., Li, S., Han, Z., Wang, T., Ma, X., & Gong, J. (2013). Hydrogen production via glycerol steam reforming over Ni/Al<sub>2</sub>O<sub>3</sub>: Influence of nickel precursors. *ACS Sustainable Chemistry and Engineering*, 1(8), 1052–1062. [https://doi.org/10.1021/SC400123F/SUPPL\\_FILE/SC400123F\\_SI\\_001.PDF](https://doi.org/10.1021/SC400123F/SUPPL_FILE/SC400123F_SI_001.PDF)
- Yahom, A., Powell, J., Pavarajarn, V., Onbuddha, P., Charojrochkul, S., & Assabumrungrat, S. (2014). Simulation and thermodynamic analysis of chemical looping reforming and CO<sub>2</sub> enhanced chemical looping reforming. *Chemical Engineering Research and Design*, 92(11), 2575–2583. <https://doi.org/10.1016/J.CHERD.2014.04.002>
- Yamaguchi, D., Tang, L., Wong, L., Burke, N., Trimm, D., Nguyen, K., & Chiang, K. (2011). Hydrogen production through methane–steam cyclic redox processes with iron-based metal oxides. *International Journal of Hydrogen Energy*, 36(11), 6646–6656. <https://doi.org/10.1016/J.IJHYDENE.2011.02.094>
- Yan, Y., Xu, L., Wang, L., Fu, K., Tang, M., Fan, M., & Ma, X. (2018). Syngas Production from Chemical-Looping Reforming of Methane Using Iron-Doped Cerium Oxides. *Energy Technology*, 6(9), 1610–1617. <https://doi.org/10.1002/ENTE.201700884>
- Yang, G., Yu, H., Peng, F., Wang, H., Yang, J., & Xie, D. (2011). Thermodynamic analysis of hydrogen generation via oxidative steam reforming of glycerol. *Renewable Energy*, 36(8), 2120–2127. <https://doi.org/10.1016/J.RENENE.2011.01.022>

- Yin, X., Shen, L., Wang, S., Wang, B., & Shen, C. (2022). Double adjustment of Co and Sr in  $\text{LaMnO}_{3+\delta}$  perovskite oxygen carriers for chemical looping steam methane reforming. *Applied Catalysis B: Environmental*, 301, 120816. <https://doi.org/10.1016/J.APCATB.2021.120816>
- Yu, Z., Yang, Y., Yang, S., Zhang, Q., Zhao, J., Fang, Y., Hao, X., & Guan, G. (2019). Iron-based oxygen carriers in chemical looping conversions: A review. *Carbon Resources Conversion*, 2(1), 23–34. <https://doi.org/10.1016/J.CRCO.2018.11.004>
- Yuan, J., Zhao, Y., Xu, H., Lu, C., Yang, K., Zhu, X., & Li, K. (2020). Layered Mg-Al spinel supported Ce-Fe-Zr-O oxygen carriers for chemical looping reforming. *Chinese Journal of Chemical Engineering*, 28(10), 2668–2676. <https://doi.org/10.1016/J.CJCHE.2020.06.035>
- Zafar, Q., Mattisson, T., & Gevert, B. (2005). Integrated hydrogen and power production with  $\text{CO}_2$  capture using chemical-looping reforming-redox reactivity of particles of CuO,  $\text{Mn}_2\text{O}_3$ , NiO, and  $\text{Fe}_2\text{O}_3$  using SiO<sub>2</sub> as a support. *Industrial and Engineering Chemistry Research*, 44(10), 3485–3496. <https://doi.org/10.1021/IE048978I/ASSET/IMAGES/LARGE/IE048978IF00011.JPEG>
- Zarei Senseni, A., Meshkani, F., Seyed Fattahi, S. M., & Rezaei, M. (2017). A theoretical and experimental study of glycerol steam reforming over Rh/ $\text{MgAl}_2\text{O}_4$  catalysts. *Energy Conversion and Management*, 154, 127–137. <https://doi.org/10.1016/J.ENCONMAN.2017.10.033>
- Zhang, Q., Jiang, B., Li, L., Liu, K., He, N., Ma, J., Zhang, X., & Tang, D. (2021). Multifunctional Ni-based oxygen carrier for  $\text{H}_2$  production by sorption enhanced chemical looping reforming of ethanol. *Fuel Processing Technology*, 221, 106953. <https://doi.org/10.1016/J.FUPROC.2021.106953>
- Zhang, Q., Li, L., Jiang, B., Wang, K., Tang, D., & Dou, B. (2017). An intelligent oxygen carrier of  $\text{La}_{2-x}\text{Sr}_x\text{NiO}_{4-\lambda}$  for hydrogen production by chemical looping reforming of ethanol. *International Journal of Hydrogen Energy*, 42(27), 17102–17111. <https://doi.org/10.1016/J.IJHYDENE.2017.05.238>
- Zhang, X., Su, Y., Pei, C., Zhao, Z. J., Liu, R., & Gong, J. (2020). Chemical looping steam reforming of methane over Ce-doped perovskites. *Chemical Engineering Science*, 223, 115707. <https://doi.org/10.1016/J.CES.2020.115707>
- Zhang, Y. ke, Zhao, Y. jie, Yi, Q., Wei, G. qiang, Shi, L. juan, & Zhou, H. (2021). NiO/ $\kappa$ - $\text{CeZrO}_4$  functional oxygen carriers with  $\text{Ni}^{2+}$  and oxygen vacancy synergy for chemical looping partial oxidation reforming of methane. *Fuel Processing Technology*, 219, 106875. <https://doi.org/10.1016/J.FUPROC.2021.106875>
- Zhao, H., Guo, L., & Zou, X. (2015). Chemical-looping auto-thermal reforming of biomass using Cu-based oxygen carrier. *Applied Energy*, 157, 408–415. <https://doi.org/10.1016/J.APENERGY.2015.04.093>
- Zhao, K., Chen, J., Li, H., Zheng, A., & He, F. (2019). Effects of Co-substitution on the reactivity of double perovskite oxides  $\text{LaSrFe}_{2-x}\text{Co}_x\text{O}_6$  for the chemical-looping steam methane reforming. *Journal of the Energy Institute*, 92(3), 594–603. <https://doi.org/10.1016/J.JOEI.2018.03.013>

- Zhao, K., He, F., Huang, Z., Wei, G., Zheng, A., Li, H., & Zhao, Z. (2016). Perovskite-type oxides  $\text{LaFe}_{1-x}\text{Co}_x\text{O}_3$  for chemical looping steam methane reforming to syngas and hydrogen co-production. *Applied Energy*, 168, 193–203. <https://doi.org/10.1016/J.APENERGY.2016.01.052>
- Zheng, X., Su, Q., Mi, W., & Zhang, P. (2014). Effect of steam reforming on methane-fueled chemical looping combustion with Cu-based oxygen carrier. *International Journal of Hydrogen Energy*, 39(17), 9158–9168. <https://doi.org/10.1016/J.IJHYDENE.2014.03.245>
- Zheng, Y., Li, K., Wang, H., Tian, D., Wang, Y., Zhu, X., Wei, Y., Zheng, M., & Luo, Y. (2017). Designed oxygen carriers from macroporous  $\text{LaFeO}_3$  supported  $\text{CeO}_2$  for chemical-looping reforming of methane. *Applied Catalysis B: Environmental*, 202, 51–63. <https://doi.org/10.1016/J.APCATB.2016.08.024>
- Zheng, Y., Li, K., Wang, H., Zhu, X., Wei, Y., Zheng, M., & Wang, Y. (2016). Enhanced Activity of  $\text{CeO}_2\text{-ZrO}_2$  Solid Solutions for Chemical-Looping Reforming of Methane via Tuning the Macroporous Structure. *Energy and Fuels*, 30(1), 638–647. [https://doi.org/10.1021/ACS.ENERGYFUELS.5B02151/ASSET/IMAGES/LARGE/EF-2015-02151M\\_0016.JPEG](https://doi.org/10.1021/ACS.ENERGYFUELS.5B02151/ASSET/IMAGES/LARGE/EF-2015-02151M_0016.JPEG)
- Zhu, L., He, Y., Li, L., & Wu, P. (2018). Tech-economic assessment of second-generation CCS: Chemical looping combustion. *Energy*, 144, 915–927. <https://doi.org/10.1016/J.ENERGY.2017.12.047>
- Zhu, M., Song, Y., Chen, S., Li, M., Zhang, L., & Xiang, W. (2019). Chemical looping dry reforming of methane with hydrogen generation on  $\text{Fe}_2\text{O}_3/\text{Al}_2\text{O}_3$  oxygen carrier. *Chemical Engineering Journal*, 368, 812–823. <https://doi.org/10.1016/J.CEJ.2019.02.197>
- Zhu, X., Li, K., Wei, Y., Wang, H., & Sun, L. (2014). Chemical-looping steam methane reforming over a  $\text{CeO}_2\text{-Fe}_2\text{O}_3$  oxygen carrier: Evolution of its structure and reducibility. *Energy and Fuels*, 28(2), 754–760. [https://doi.org/10.1021/EF402203A/ASSET/IMAGES/LARGE/EF-2013-02203A\\_0009.JPEG](https://doi.org/10.1021/EF402203A/ASSET/IMAGES/LARGE/EF-2013-02203A_0009.JPEG)
- Zhu, X., Wang, H., Wei, Y., Li, K., & Cheng, X. (2011). Hydrogen and syngas production from two-step steam reforming of methane using  $\text{CeO}_2$  as oxygen carrier. *Journal of Natural Gas Chemistry*, 20(3), 281–286. [https://doi.org/10.1016/S1003-9953\(10\)60185-5](https://doi.org/10.1016/S1003-9953(10)60185-5)
- Zhu, X., Wei, Y., Wang, H., & Li, K. (2013). Ce–Fe oxygen carriers for chemical-looping steam methane reforming. *International Journal of Hydrogen Energy*, 38(11), 4492–4501. <https://doi.org/10.1016/J.IJHYDENE.2013.01.115>